NV5 GEOSPATIAL

Survey: September 1-4, 2022
Report: Feb 13, 2023 (REV)

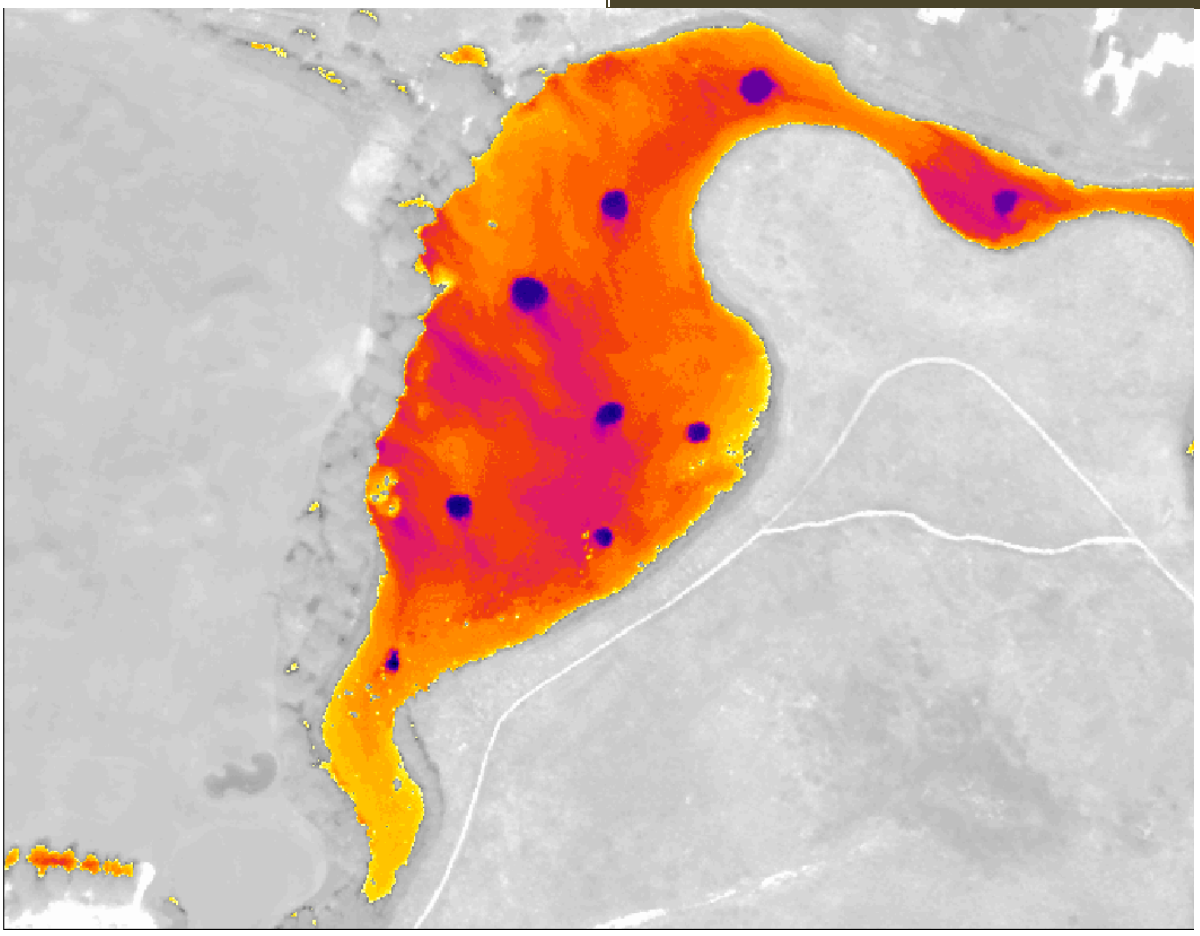

Salmon Streams, OR Technical Data Report
Airborne Thermal Infrared and True Color Imagery

Prepared for:

USDA

Mark Riley
Edith Green Bldg 1405
1220 SW 3rd Ave
Portland, OR 97204

Prepared by:

NV5 GEOSPATIAL

NV5 Geospatial
1100 NE Circle Blvd, Ste. 126
Corvallis, OR 97330
PH: 541-752-1204

TABLE OF CONTENTS

INTRODUCTION 1
Deliverable Products 2
DATA ACQUISITION 4
Acquisition planning and Execution 4
Flight Planning 4
Thermal Infrared Sensor: FLIR x8501SC SLS 4
True Color Sensor 6
In Stream Temperature Sensors 7
Executing Airborne Thermal Infrared Acquisition 9
DATA PROCESSING 11
Thermal Infrared Data Processing 11
Thermal Infrared Imagery Calibration 11
TIR Mosaic Generation 11
True Color (RGB) Mosaic Generation 12
Temperature and Color Ramps 13
Accuracy Assessment Methodology 14
Interpretation and Feature Extraction 15
Stream Centerlines 15
Longitudinal Temperature Profiles 15
Significant Thermal Features 15
Calculated Statistical Parameters 15
ANALYSIS RESULTS 19
Thermal Infrared Data Processing 19
Accuracy Assessment Results 19
North Fork Siuslaw River, McLeod Creek 20
McKenzie River, Quartz Creek, Cone Creek, Ennis Creek 22
South Fork McKenzie River and McKenzie River (Section A) 24
Deer Creek and McKenzie River (Section b) 26
Whychus Creek 29
Indian Ford Creek 34
Fivemile Creek and Bell Creek 36

True Color Orthophoto Accuracy Assessment 39

Cover Photo: Thermal infrared imagery of Indian Ford Creek survey area.

Thermal infrared imagery was processed and reported by:
Mousa Diabat, Ph.D. - Hydrologist, Thermographer Level 3
Chris Miwa - Certified Photogrammetrist.

FIGURES

Figure 1: AOI location map of the Salmon Stream project in western Oregon. 3
Figure 2: Installation setup of FLIR x8501SC SLS in the fixed-wing aircraft used for Salmon Streams project. 5
Figure 3: Water temperature data logger that was used for the project. Brand and model: HOBO Water Temperature Pro V2 ONSET U22-001. 7
Figure 4: Map of the Whychus Creek AOI and the site of the temperature data loggers (green). 8
Figure 5: This image shows an example of the position of the data logger based on a handheld GPS unit (green) and its adjusted position based on field crew description and final TIR mosaic (blue). 9
Figure 6: Flight lines covering Whychus Creek AOI. 10
Figure 7: Examples of different color ramps applied to the same TIR image. 14
Figure 8: TIR image shows an example of one LTP sampling point that fell on a bridge crossing the river. This point, for an example, can be excluded from the final LTP data by the user. 16
Figure 9: TIR image shows an example of sampling points along the centerline within the predefined buffer. 17
Figure 10: An examples of significant thermal features (STFs) that identify a potential inflow from a side channel or cold-water spring flowing into the main channel. 17
Figure 11: NF Siuslaw River and McLeod Creek survey area. 20
Figure 12: LTP of NF Siuslaw River showing the downstream warming and cooling gradients. The plot shows median water temperature (°C). 21
Figure 13: The confluence of McLeod Creek with NF Siuslaw River showing the latter was 1.5 °C warmer. 21
Figure 14: McKenzie River survey area (main section). 22
Figure 15: LTP of the McKenzie River showing the downstream warming gradient (12.6 to 13.3°C) between river km 8 and 4.8 where Quartz Creek flows in. The river water temperature stabilized for the rest of the surveyed section. The plot shows median water temperature (°C). 23
Figure 16: The confluence of Quartz Creek with the McKenzie River showing temperature difference of nearly 7 °C. 23
Figure 17: The confluence of Ennis Creek with the McKenzie River showing temperature difference of nearly 7 °C. 24
Figure 18: South Fork McKenzie River survey area. 25
Figure 19: LTP of the SF McKenzie River showing the downstream warming gradient (14.0 to 15.9°C) within 2.3 km of the surveyed area. The plot shows median water temperature (°C). 25
Figure 20: The impact of warm water inflow from the SF McKenzie River into the mainstem McKenzie River causing 1.8 ^{o}C warming of the later. 26
Figure 21: Deer Creek survey area. 27
Figure 22: LTP of Deer Creek showing the stead downstream warming gradient along its 3.1 km channel length. Water temperature increased from 14 °C to nearly 20 °C by the time it flowed into the McKenzie River. The warm water inflow from Deer creek cause a slight warming to the McKenzie River from 10.0 °C to 10.7 °C. The plot shows median water temperature (°C). 28
Figure 23: The impact of warm water inflow from Deer Creek into the McKenzie River causing 0.7 ^{o}C warming of the later. 29

Figure 24: Whychus Creek survey area. 30
Figure 25: LTP of Whychus Creek showing the downstream warming gradient along river section 6.2 to 2. Water temperature increased from lower than 18 °C to over 21 °C. Water temperature along lower 2 km of the surveyed section remained relatively steady between 21 and 22 °C. The plot shows median water temperature (°C). 31
Figure 26: LTP and STF data overlaying TIR data. The identified STF was nearly 1 °C lower than the water in the channel representing a potential hyporheic exchange zone or a small spring. 32
Figure 27: LTP and STF data overlaying TIR data. The identified STF of the side channel was nearly 1 °C warmer than the water in the channel. 33
Figure 28: Indian Ford Creek survey area. 34
Figure 29: LTP data overlaying TIR data along the headwaters of Indian Creek. 35
Figure 30: LTP data overlaying TIR data along the aerated ponds. 35
Figure 31: LTP of Indian Ford Creek showing the downstream warming gradient along river section 6.1 to 3.6. The fluctuation along the middle section here is a result of the lack of water mixing found in the ponds along the surveyed channel. The section downstream of river km 3.6 was too narrow and had low flow preventing the generation of a proper LTP plot. The plot shows median water temperature (°C). .. 36
Figure 32: Fivemile Creek and Bell Creek survey area. 37
Figure 33: LTP overlayed on top of TIR data showing Bell Creek flowing into Fivemile Creek. This figure shows the patches of exposed water surface along the stream. The plot shows median water temperature (°C). 38
Figure 34: LTP overlayed on top of TIR data of Fivemile Creek at river km 0.55. This figure shows a continuous thermal signature of the active channel at the lower end of the surveyed area. The plot shows median water temperature (°C). 38

TABLES

Table 1: Acquisition dates, acreage, and data types collected on the Salmon Streams site 1
Table 2: Products delivered to the USFS, Pacific Northwest Region (R6) 2
Table 3: Summary of TIR sensor and acquisition specifications 5
Table 4: Camera manufacturer's specifications 6
Table 5: Project-specific orthophoto specifications 6
Table 6: Processing steps for TIR mosaic generation 12
Table 7: Orthophoto processing workflow 13
Table 8: Summary of the processing and analyses steps used in the thermal analysis 18
Table 9: Summary of accuracy assessment values. 19
Table 10: List of surveyed tributaries and their lengths. 20
Table 11 List of surveyed tributaries and their lengths. 22
Table 12 List of surveyed tributaries and their lengths. 24
Table 13 List of surveyed tributaries and their lengths. 27
Table 14 List of surveyed tributaries and their lengths. 29
Table 15 List of surveyed tributaries and their lengths. 34
Table 16 List of surveyed tributaries and their lengths. 36
Table 17: Orthophotography accuracy statistics for Salmon Streams 39

INTRODUCTION

NV5 Geospatial was contracted by the USFS, Pacific Northwest Region (R6) to collect airborne thermal infrared (TIR) and true color imagery (RGB) for the Salmon Streams project during the summer of 2022. The survey targeted seven areas of interest (AOIs) located throughout western and central Oregon encompassing nearly 4,000 acres. The purpose of this survey was to aid the USFS, Pacific Northwest Region (R6) with ongoing stream and riparian monitoring and restoration efforts.

This report accompanies the delivered TIR and RGB data and support files, and documents contract specifications, data acquisition procedures, processing methods, and analysis of the final datasets. Acquisition dates and acreage are shown in Table 1, deliverables provided to USFS, Pacific Northwest Region (R6) and projection information are shown in Table 2, and the project extent is shown in Figure 1.

Table 1: Acquisition dates, acreage, and data types collected on the Salmon Streams site

Project Site	Contracted Acres	Buffered Acres	Acquisition Dates	Data Type
Salmon Streams, Oregon	3,036	3,997	09/01/2022 09/02/2022 09/04/2022	3 band (RGB) Digital Imagery Thermal Infrared Imagery

Deliverable Products

Table 2: Products delivered to the USFS, Pacific Northwest Region (R6)

Salmon Streams TIR and RGB 2022 Products Projection: USFS R6 Albers Horizontal Datum: NAD83(2011) Vertical Datum: NAVD88 (GEOID12B) Spatial Units: meter – Temperature Units: Celsius	
Rasters	Thermal Infrared Imagery at 0.3 m resolution (*.tif): • Calibrated image files (cell values = Celsius x 10) • Calibrated imagery mosaics by mission (cell values = Celsius x 10) True Color (RGB) Imagery Mosaics (10 cm) • Tiled geotiffs (*.tif) • AOI compression (*.sid)
Vectors	Shapefiles (*.shp) • Project survey boundary • Temperature data loggers' location • TIR image center points and sensor exterior orientation (EO) • Stream centerlines • Longitudinal temperature profile (LTP) • Significant thermal features (STF) • True Color (RGB) imagery tile index • True Color (RGB) image center points • Air Target Points
Analysis	• Longitudinal temperature profiles ("LTP_STF", *.xlsx) • Customized layer files for an improved visualization ("Color Ramps", *.lyr)
Report	• Technical report • "Maps and Figures" folder containing maps and figures used for the report

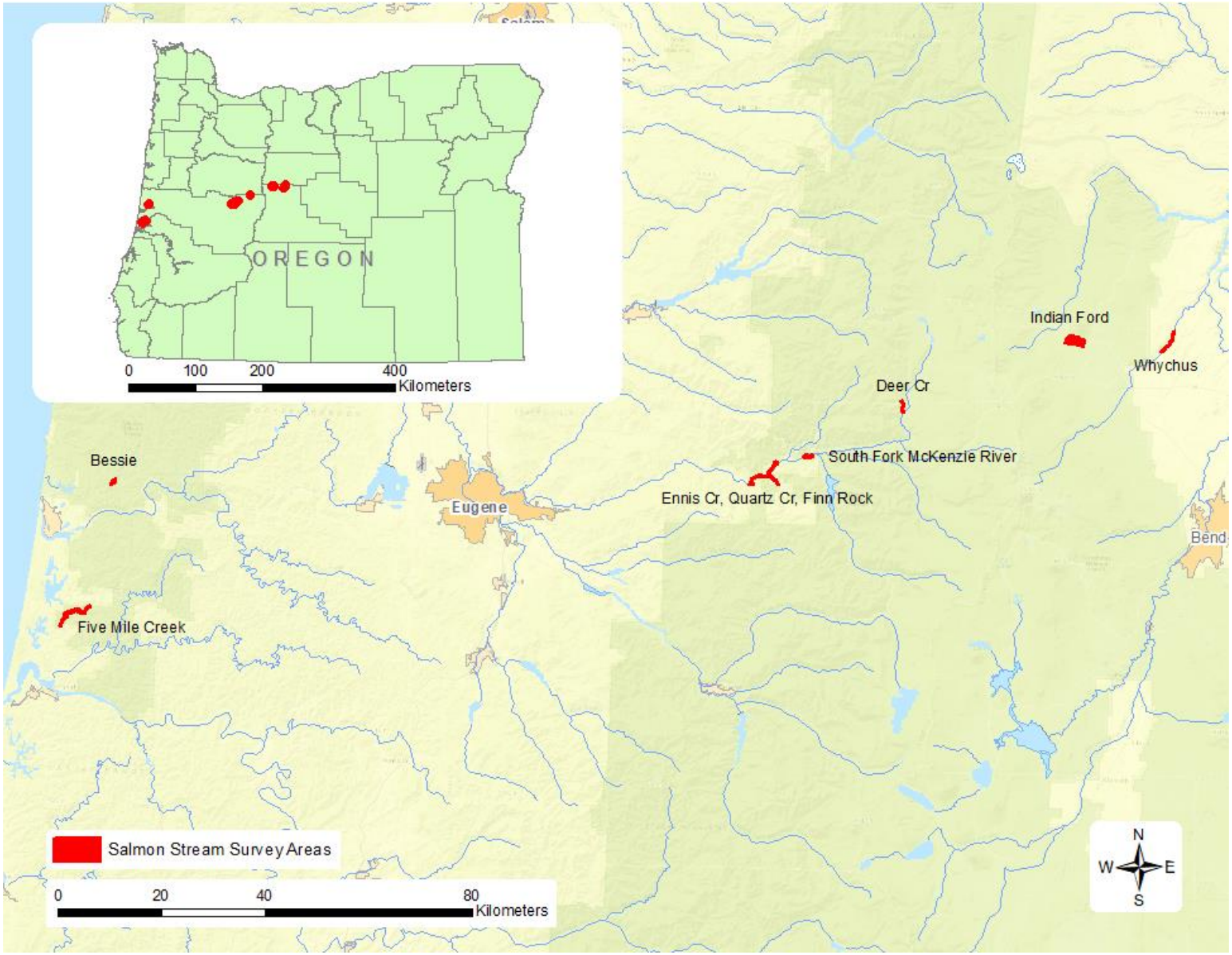

Figure 1: AOI location map of the Salmon Stream project in western Oregon.

Acquisition planning and Execution

Flight Planning

In preparation for data collection, NV5's crew reviewed the project area and developed a specialized flight plan to ensure complete coverage of the Salmon Streams survey area. The TIR acquisition flights were scheduled for an afternoon time window to maximize temperature contrast between thermal signatures of water in the river channel, features across the floodplain, and those along the riparian zone. Atmospheric conditions and the diurnal fluctuation of stream temperatures dictate that TIR data should be acquired in a limited time window to avoid temperature variation between the beginning and the end of the acquisition flight. The flight plan was designed so the aircraft flies in parallel and opposing flight lines follows the stream pathway at an altitude of 400 meters above ground level (AGL) to achieve a ground sample distance of ≤ 0.5 meter.

Weather forecasts prior to the survey date were closely monitored for favorable conditions. Ideal weather conditions consist of low-to-mid range relative humidity, warm and sunny days, and cloud-free skies. Precipitation was also monitored in and around the survey area. TIR acquisition should not occur earlier than 72 hours following any rain event greater than 0.5 inch. Ideal weather conditions reduce the chances for masking the thermal signature of significant features by cool air temperatures, clouds, or increased river flow. Because water has higher heat capacity and emissivity than the gravel and rock across the floodplain, under the same conditions of solar loading the river's temperature increase at a lower rate than it is surrounding. These physical characteristics improve the thermal contrast under the right conditions.

Thermal Infrared Sensor: FLIR x8501SC SLS

NV5 used a FLIR X8501SC with a spectral range of 7.5 – 12.0 μm which was mounted to a fixed-wing single-engine Cessna 208B owned by NV5 (tail number N473TW). was installed in the aircraft's floor in designated opening for the down-facing lens (Figure 2). The TIR sensor uses a focal plane array of detectors to sample incoming radiation based on the technology of Quantum Well Infrared Photodetector (QWIP). The sensor's array records the change of state of electrons in a crystal structure reacting to incident photons. This technology is faster and more sensitive than polymer thermal detectors. A cooling mechanism is required for this sensor to stabilize its internal temperature and minimize thermal drift during acquisition. To achieve uniformity across the detector array, a factory scheme is generated to reduce non-uniformity across the image frame. Differences in temperature (typically <0.5° C) might be observed near the edge of the image frame. Flight planning ensures sufficient image overlap so that frame edges can be excluded from the river channel in the TIR image mosaics. The resulting thermal infrared image frames were recorded directly from the sensor to an on-board computer as raw photon counts which were then converted to radiant temperatures. Sensor and acquisition specifications for the Salmon Streams TIR study are listed in Table 3.

Table 3: Summary of TIR sensor and acquisition specifications

FLIR System x8501SC SLS (LWIR)	
Wavelength:	7.5 – 12.0 μm
Noise Equivalent Temperature Differences (NETD):	0.035 °C
Pixel Array:	1280 (H) x 1024 (V)
Encoding Level:	14 bit
Horizontal Field-of-View:	17°x14°
Sensor Focal Length	50 mm
Acquisition Dates:	September 1-2 & 4, 2022
Planned Flying Height Above Ground Level (AGL):	400 meter
Image Ground Footprint Width:	600 meter
Ground Sampling Distance (GSD)	≤ 0.5 meter

Figure 2: Installation setup of FLIR x8501SC SLS in the fixed-wing aircraft used for Salmon Streams project.

Similar to all thermal infrared sensors, the FLIR sensor only detects the radiation received from the surface of the object. In the case of surveying rivers and stream, it is assumed that the water column is fully mixed and the heat signature at the surface represents the temperature of the water column. Thermal infrared radiation detected by the sensor is the sum of the longwave radiation forms: emitted, reflected and transmitted. Thermal signature that is registered by the sensor for water I the river is mostly emitted by the water because of its high emissivity (0.96-0.98), while only 2% is reflected and 0% is transmitted (water is opaque to longwave range).

To accurately georeference the TIR imagery, the positional coordinates of the airborne sensor and the orientation of the aircraft were recorded continuously throughout the data collection missions. Position and altitude of the aircraft was measured twice per second (2 Hz) by an onboard differential GPS unit, while pitch, roll, and yaw (heading) were measured 200 times per second (200 Hz) from an onboard inertial measurement unit (IMU). To allow for post-processing correction and calibration, aircraft/sensor position and attitude data are indexed by GPS time.

True Color Sensor

True color (RGB) imagery was co-acquired (with the thermal infrared and LiDAR data) using a PhaseOne iXM-100F digital camera (Table 4). The PhaseOne is a medium format aerial mapping camera which collects imagery in three spectral bands (Red, Green, Blue).

Table 4: Camera manufacturer's specifications

Parameter	PhaseOne iXM-100F Specification
Focal Length	70 mm
Spectral Bands	Red, Green, Blue
Pixel Size	4.6 µm
Image Size	11,608 x 8,708 pixels
Frame Rate	GPS triggered
FOV	43° x 32°
Data Format	8bit TIFF

For the Salmon Streams site, 4,414 images were collected in three spectral bands (red, green, blue) with 60% along track overlap and 50% sidelap between frames. The acquisition flight parameters were designed to yield a native pixel resolution of ≤ 0.1 m. Orthophoto specifications particular to the Salmon Streams project are in Table 5.

Table 5: Project-specific orthophoto specifications

Parameter	Digital Orthophotography Specification
Ground Sampling Distance (GSD)	≤ 0.1 m
Along Track Overlap	≥60%
Cross Track Overlap	≥50%

Parameter	Digital Orthophotography Specification
Height Above Ground Level (AGL)	400 m
GPS PDOP	≤3.0
GPS Satellite Constellation	≥6

In Stream Temperature Sensors

A total of 7 data loggers (Figure 3) recording water temperature were deployed by NV5's field crew at specified sites across the Salmon Streams survey areas (example in Figure 4). Data loggers recorded water temperature throughout the survey period at 10-minute intervals. Data from the data loggers were used in the radiometric calibration process.

Figure 3: Water temperature data logger that was used for the project. Brand and model: HOBO Water Temperature Pro V2 ONSET U22-0011.

The field crew adheres to the following list of guidelines for deploying the data loggers:

1) In well mixed, flowing waters section of the river or stream and not in pools or riffles sections.
2) In a water column deeper than 0.5 meter and shallower than 2 meters to allow for fully submerged data loggers and avoid a stratified water column.
3) Within the channel's thalweg to measure a larger bulk of flowing water in the stream.
4) In a water body with a sufficiently exposed surface to the sky that can be detected by the sensor mounted to the aircraft.
5) Away from the bank where riparian vegetation may block the view from the aircraft.
6) In water stream reaches free from above-water surface features such as boulder and riparian and aquatic vegetation to allow for uniform water temperatures across the stream or the water body.

[1] https://www.onsetcomp.com/products/data-loggers/u22-001

7) Avoid deploying the sensor in shallow waters where it can be exposed to direct sun light. Sensors under direct sun light heat up and skew the recorded temperature.

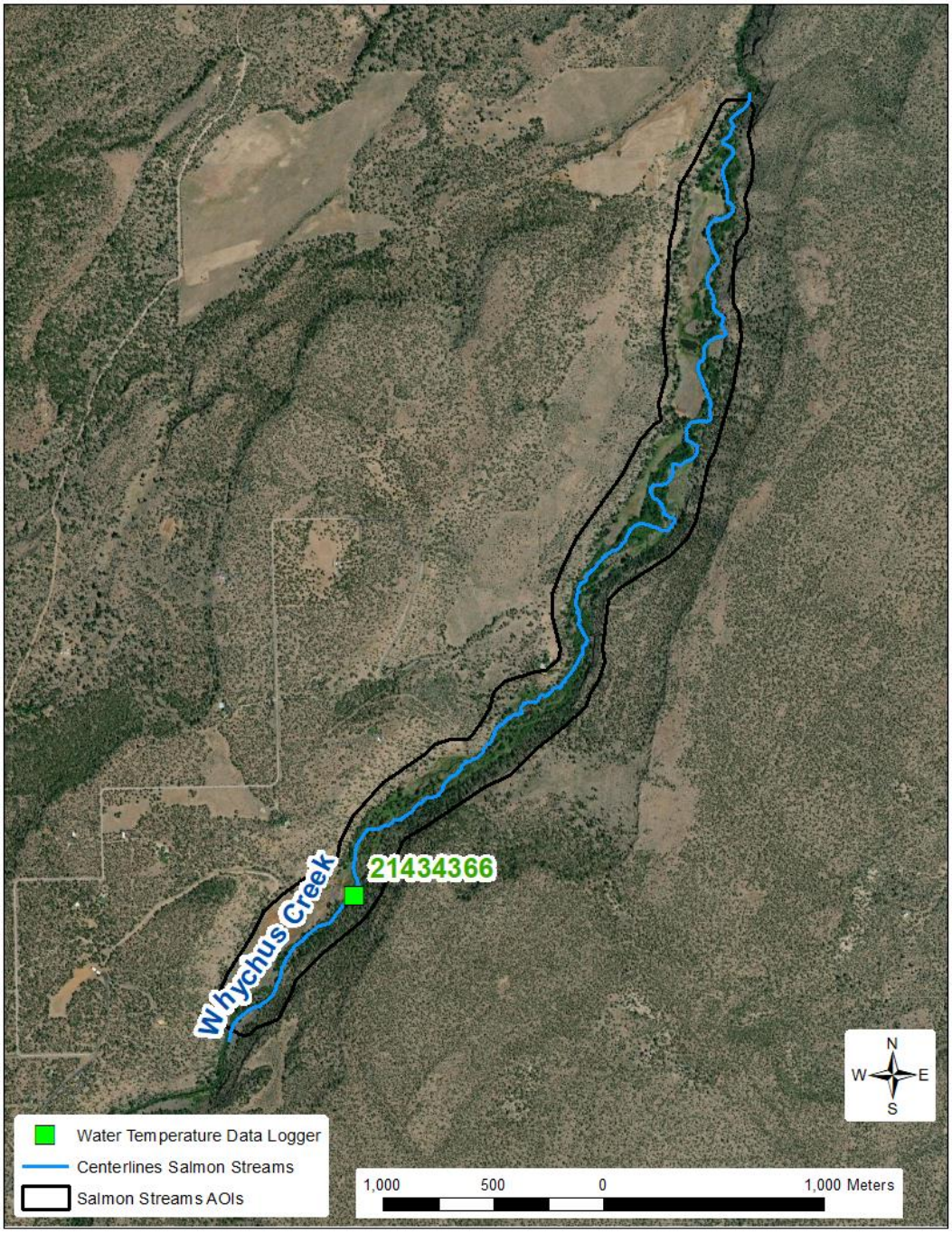

Figure 4: Map of the Whychus Creek AOI and the site of the temperature data loggers (green).

Positioning the data logger following above guidelines is essential to achieve the best radiometric calibration and imagery mosaic possible. It is scientifically sound to assume a thoroughly mixed water column in flowing stream and rivers no deeper than 4 meter. Additionally, deploying the sensor in shallow water, exposed to direct sun light has the potential to skew the recorded temperature by representing the temperature of the streambed, or the sensor itself, that has been absorbing heat all day.

Assessing the TIR mosaic's accuracy becomes challenging when temperature values are highly variable around the logger position. In this case there may be "blended pixels" in the TIR mosaic representing two or more objects with varying temperatures, i.e., water and non-water features. Examples of such instances are narrow channels, obscured water surface by above-water surface boulders and vegetation (riparian or aquatic), and the mixing zone of entering tributaries or point-source inflow.

The logger's position is recorded by using a handheld GPS unit which can have a small spatial inaccuracy up to a few meters. This error can cause problems during temperature calibration if there are large differences in water temperature between the GPS position and actual position of the data logger. Adjusting the position relies on information from the field crew, or the client if the latter is providing the data, to accurately position the logger in the stream (Figure 5).

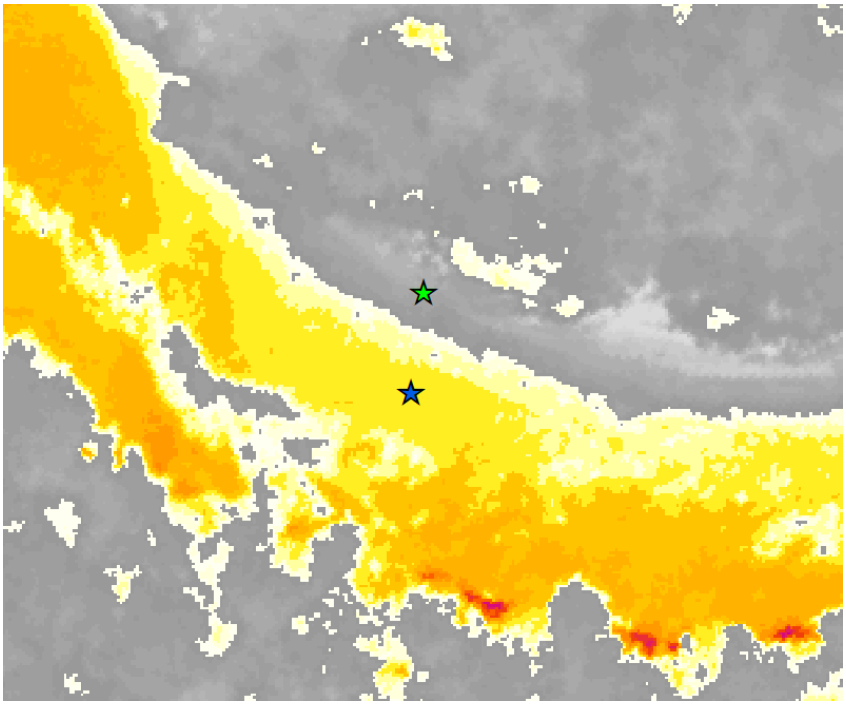

Figure 5: This image shows an example of the position of the data logger based on a handheld GPS unit (green) and its adjusted position based on field crew description and final TIR mosaic (blue).

Executing Airborne Thermal Infrared Acquisition

The data were acquired during the afternoon hours on September 1, 2, and 4, 2022. The aircraft was flown in parallel and opposing flight lines at the targeted flight altitude of 400 meters above ground level to achieve a ground sample distance of ≤ 0.5 m. TIR flight lines are shown in Figure 6.
The TIR sensor was set to acquire images at a rate of 1 image per second (1 Hz) resulting in 60% or greater forward overlap between images. Thermal infrared images were recorded directly from the sensor to an on-board computer as raw digital numbers (to be converted to radiant temperature during the radiometric calibration step). The individual images were referenced with timestamp, position, and heading information provided by an onboard survey-grade global positioning system (GPS).

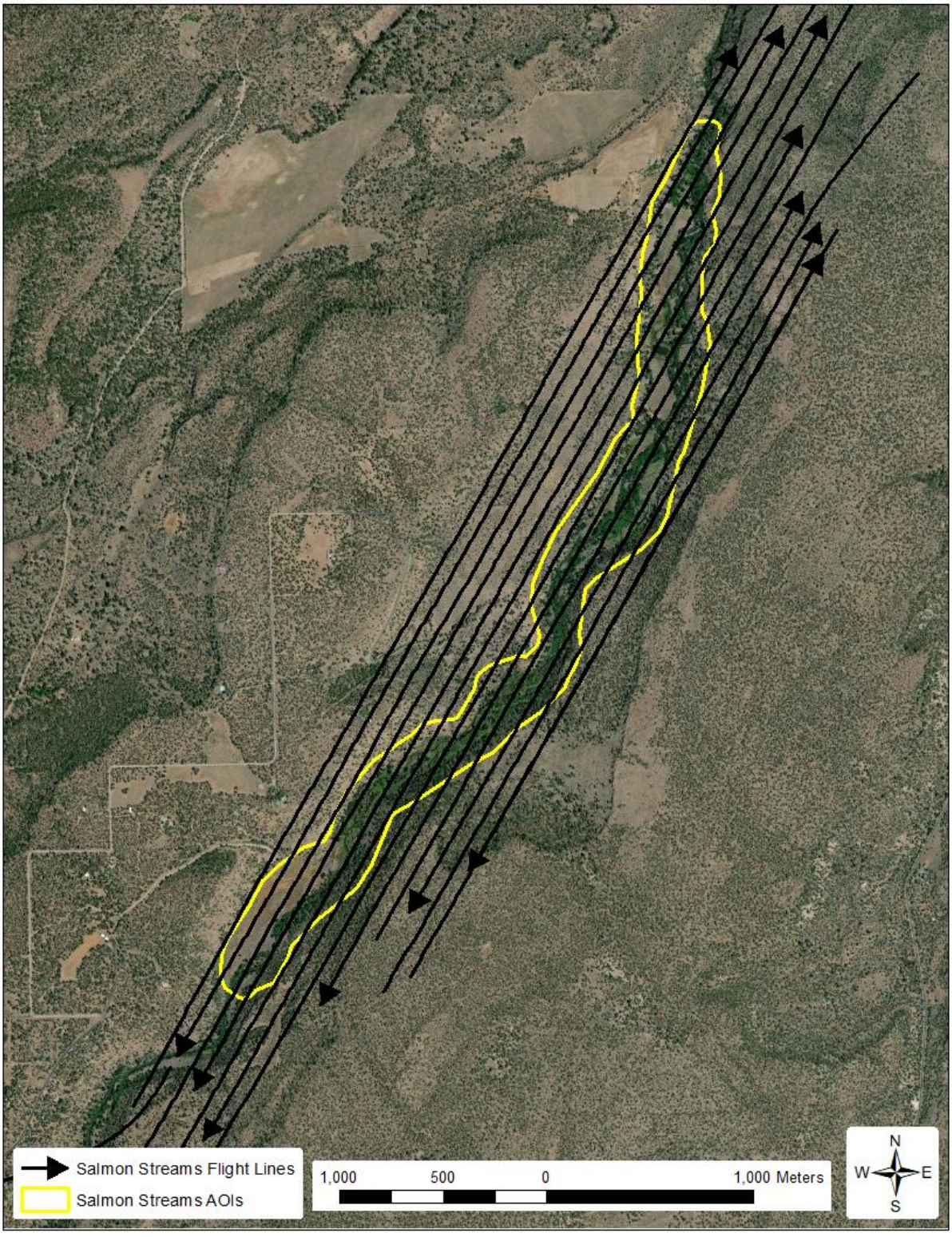

Figure 6: Flight lines covering Whychus Creek AOI.

Thermal Infrared Data Processing

Thermal Infrared Imagery Calibration

The process of TIR calibration connects the thermal radiation recorded by the FLIR sensor and the kinetic temperature of the targeted object which was measured by the in-stream data loggers. Response curves of the TIR sensor were measured in a laboratory environment as part of the periodic maintenance procedure stated by the sensor's manufacturer. In laboratory environment, the sensor records thermal infrared radiation emitted by a black body as digital numbers which were used to generate the response curves. All objects have physical parameters of emitting, reflecting, and transmitting radiation with varying values as the following equation shows:

$$emissivity + reflectivity + transmisivity = 1$$

In theory, a black body has an emissivity (e) value of 1.0, and reflectivity (r) and transmissivity (t) values of 0.0. However, the TIR calibration is based on the recorded temperature of water which has emissivity value of 0.98[2], reflectivity value of 0.02, and transmissivity value of 0.0. The water surface reflects thermal radiation of the atmosphere, while the water column is opaque and does not transmit radiation in the longwave thermal spectrum.

The process of thermal calibration adjusted for the distance between the water and the sensor and accounted for atmospheric conditions (relative humidity and ambient temperature) in order to adjust radiance at the sensor based on the kinetic temperatures recorded by water temperature data loggers. Imagery from flight lines that did not cover data loggers, were calibrated based on overlapping imagery from adjacent lines, a technique that is referred to as "line-to-line calibration". Minor deviations from the initial calibration might be needed to achieve the best possible temperature continuity possible throughout the mosaic.

TIR Mosaic Generation

Initially, a boresight calibration flight was processed to calculate the misalignment angles between the sensor and IMU system; this step allows for direct georeferencing of imagery without aerial triangulation. For each production flight, a series of corrections were applied to the aircraft trajectory and orientation using Applanix PP-RTX processing methodologies. Image timestamps were linked to the corrected trajectory to resolve the exterior orientation (EO) of the sensor for each image event. The resulting EO, sensor interior orientation (IO), and calibrated TIR images were input into Inpho's OrthoMaster software to generate orthophotos using a publicly available digital elevation model (DEM). Finally, for the TIR ortho images, a mosaic was generated without applying color balancing and minimal seam line feathering to preserve the original temperature values of the TIR imagery as best possible. Processing steps and software used are detailed in Table 6.

[2] Baldridge, A. M., S.J. Hook, C.I. Grove and G. Rivera, 2009. The ASTER Spectral Library Version 2.0. Remote Sensing of Environment, vol 113, pp. 711-715.

Table 6: Processing steps for TIR mosaic generation

Orthophoto Processing Step	Software Used
Calculate camera misalignment angles from a system boresight flight conducted close to survey area.	Applanix CalQC v8.7
Resolve kinematic corrections for aircraft position data using kinematic aircraft GPS and static ground GPS data. Develop a smoothed best estimate of trajectory (SBET) file that blends post-processed aircraft position with sensor head position and attitude recorded throughout the survey.	Applanix POSPac MMS v8.7
Calculate exterior orientation (EO) for each image event by linking the event time stamps with the SBET and boresight misalignment angles.	Applanix POSPac MMS v8.7
Convert raw (*.ats) TIR data into thermally calibrated TIFF images.	Examine IR v4.4
Import DEM and generate individual ortho images.	Inpho OrthoMaster v10.1
Mosaic orthorectified imagery, generating seams between individual photos.	OrthoVista v10.1

True Color (RGB) Mosaic Generation

The collected RGB imagery went through multiple processing steps to create final orthophoto products. Initially, images were geometrically corrected for lens distortion using camera calibration parameters and output as 8bit tiff images. Photo position and orientation were then calculated by linking the time of image capture to the smoothed best estimate of trajectory (SBET) file created during lidar post-processing. Within Inpho Match AT, an automated aerial triangulation was performed to refine camera exterior orientations and adjust the photo blocks to align with ground control.

Adjusted images were orthorectified using the lidar-derived ground model to remove displacement effects from topographic relief inherent in the imagery and individual orthorectified TIFFs were blended together to remove seams. The final mosaics were corrected for any remaining radiometric differences between images using Inpho's OrthoVista. The processing workflow for orthophotos is summarized in Table 7.

Table 7: Orthophoto processing workflow

Orthophoto Processing Step	Software Used
Resolve kinematic corrections for aircraft position data using kinematic aircraft GPS and static ground GPS data. Develop a smoothed best estimate of trajectory (SBET) file that blends post-processed aircraft position with sensor head position and attitude recorded throughout the survey.	POSPac MMS v.8.7
Generate camera exterior orientations (EO) by linking image events with the SBET file, resulting orientations are in Omega, Phi, Kappa representing the image coordinate system.	POSPac MMS v.8.7
Convert raw imagery data into geometrically corrected TIFF images.	iX Capture v3.4
Apply EO to photos, and perform aerial triangulation using automatically generated tie points and ground control data.	Inpho Match AT v10.1
Import DEM and orthorectify image frames	Inpho OrthoMaster v10.1
Mosaic orthorectified imagery blending automated and manually drawn seams between photos and applying global color balancing to the project.	Inpho OrthoVista/Seameditor v10.1

Temperature and Color Ramps

The final TIR mosaic contains pixel values of degrees Celsius multiplied by 10, stored in a 16bit unsigned integer raster format. Temperature values occupy a relatively narrow range of the full 16bit histogram; thus, visual representation of the imagery is enhanced by the application of a customized color ramp. Color ramps also highlight different features relevant to the analysis, such as spatial variability of stream temperatures and inflows (Figure 7). The color ramps for the TIR mosaics were developed to maximize contrast for most surface water features and are unique to each tributary or mosaic. A TIR specialist at NV5 customized unique color ramps to improve visual presentation of the TIR mosaic and exported the color ramps as ESRI layer files (*.lyr). Color ramps are an important product that is delivered to the end user.

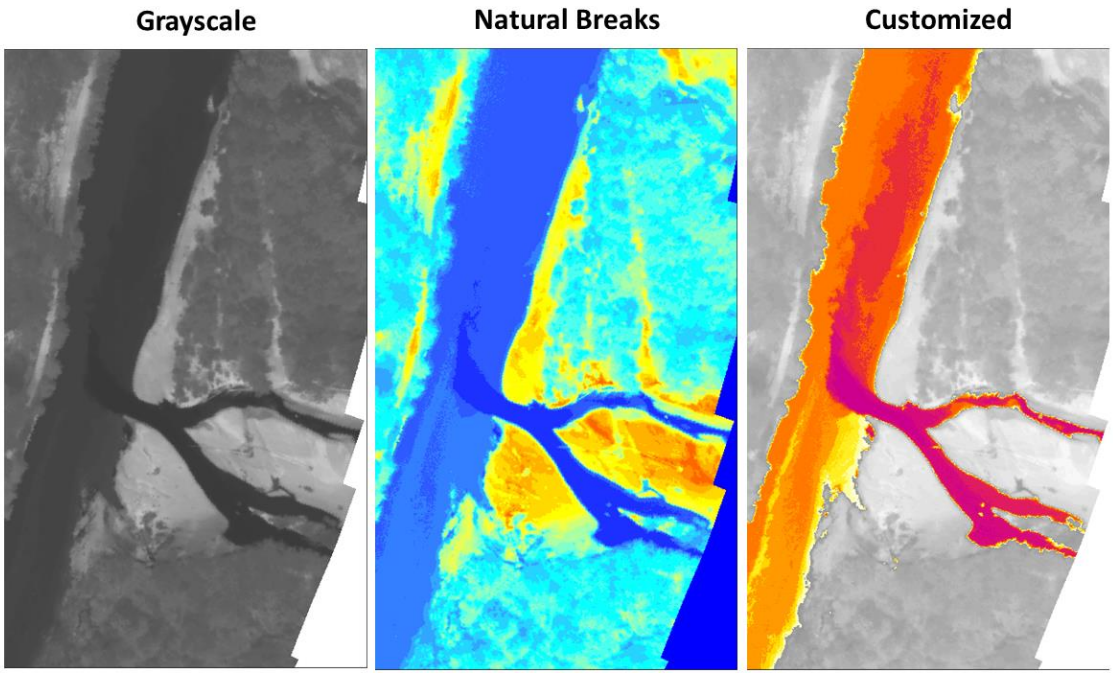

Figure 7: Examples of different color ramps applied to the same TIR image.

Accuracy Assessment Methodology

The radiometric accuracy of the final TIR mosaic was assessed by comparing sampled pixels of the mosaic (where water features were present) at the data logger locations against the temperature recorded by the respective logger.

The goal was to reach a mean absolute error (MAE) of ≤1.0 °C temperature difference between the mosaic and logger-recorded values at the time of acquiring the TIR imagery. The threshold of MAE ≤1.0 °C accounts for impeded errors of the data logger (≤0.2 °C) and the FLIR sensor (≤0.035 °C). Collecting the data in the shortest time window possible is advantageous to avoid deviation from calibrated values due to the natural diurnal fluctuation of rivers. Furthermore, the mosaic's accuracy relies on the recorded temperatures and deployment conditions of the data loggers.

Assessing the mosaic's accuracy becomes challenging if the logger is positioned where there is no cluster of pixels with uniform temperatures in the mosaic. Such sites lead to "blended pixels" in the TIR mosaic. A blended pixel is one that represents two or more objects with varying temperatures, i.e., water and non-water features. Examples of such sites are narrow channels, water surfaces obscured by above-surface boulders and vegetation (riparian or aquatic), and the mixing zone of tributaries or point-source inflow. NV5's protocol of deploying temperature data loggers includes guidance to avoid such sites.

Interpretation and Feature Extraction

To begin interpretation of thermal infrared data, a trained analyst reviewed the final mosaics to obtain a detailed understanding of the temperature distribution across the survey area. An emphasis was put on identifying the thermal signature of water bodies and streams. This was also the first step in identifying the thermal signature and location of potential inflow sources of cold/hot water. The analysis generates 3 products: stream centerlines, longitudinal temperature profiles, and significant thermal features. Data analysis and sampling tools are listed in Table 8.

Stream Centerlines

A stream centerline was digitized for each of the identifiable channels based on the TIR mosaics (*at a scale of 1:5,000*). As the centerline was digitized, care was taken to avoid non-water features where possible, such as aquatic vegetation, boulders, and overhanging canopy. However, a few non-water features cannot always be avoided, such as bridges. River length was measured cumulatively from the most downstream point in the area of interest (AOI) towards the most upstream point. Therefore, the calculated length represents only the streams within the surveyed AOI and is not relative to the overall river network outside the AOI. The centerline is stored as geospatial data file format (ESRI shapefile).

Longitudinal Temperature Profiles

The longitudinal temperature profile (LTP) is generated by sampling the TIR mosaic at equal intervals along the digitized centerlines. The LTP contributes to interpretation of the temperature gradient along the stream. The sampling is conducted using a proprietary algorithm and stores the results in a geospatial data file format (ESRI shapefile) and in a tabular format and plots of water temperature against river distance. For each point of the LTP, the algorithm extracts the pixel values from the TIR mosaic at 10 points along the centerline within a specified distance from the LTP point (Figure 8 and Figure 9). The summary includes statistical parameters of mean, median, maximum, minimum, and standard deviation. The statistical information is used to identify sampling points that fall on non-water features such as boulders or bridges.

Significant Thermal Features

The significant thermal features (STF) are thermal anomalies that were manually identified in the TIR mosaic and linked to potential inflows from natural sources or otherwise, hyporheic inflow, or tributaries. A proprietary algorithm was used to extract values of all pixels inside a specified buffer area (Figure 10). For each STF, temperature results were summarized in statistical parameters of mean, median, maximum, minimum, and standard deviation of the pixels inside the buffer. The algorithm also measured their distance from the centerline and attributes them with a river mark along the centerline (closest point on the centerline). The STF sampling results were stored in a geospatial data file format (ESRI shapefile) and plotted against river distance with the LTP results.

Calculated Statistical Parameters

The statistical parameters summarize the temperature values of all 10 sample points for the LTP and all pixels inside the buffered area for the STF.

- Mean and median: define the mean and median temperature values of all 10 sampled points/pixels.
- Minimum and maximum: define the minimum and maximum temperature values among all points/pixels. The minimum is used to plot STF results where the interest is to identify cold inflow and the maximum is used to identify hot inflow.
- Standard deviation: defines the standard deviation across all sampled points/pixels. This value is important to identify sample points that represent non-water features. A low standard deviation indicates homogeneous thermal features among the sample points and a high standard deviation indicates that the set of sample points includes features (e.g., exposed rocks/boulders) with temperature significantly different than the water body. The value of standard deviation is important for identifying and removing invalid sample points.

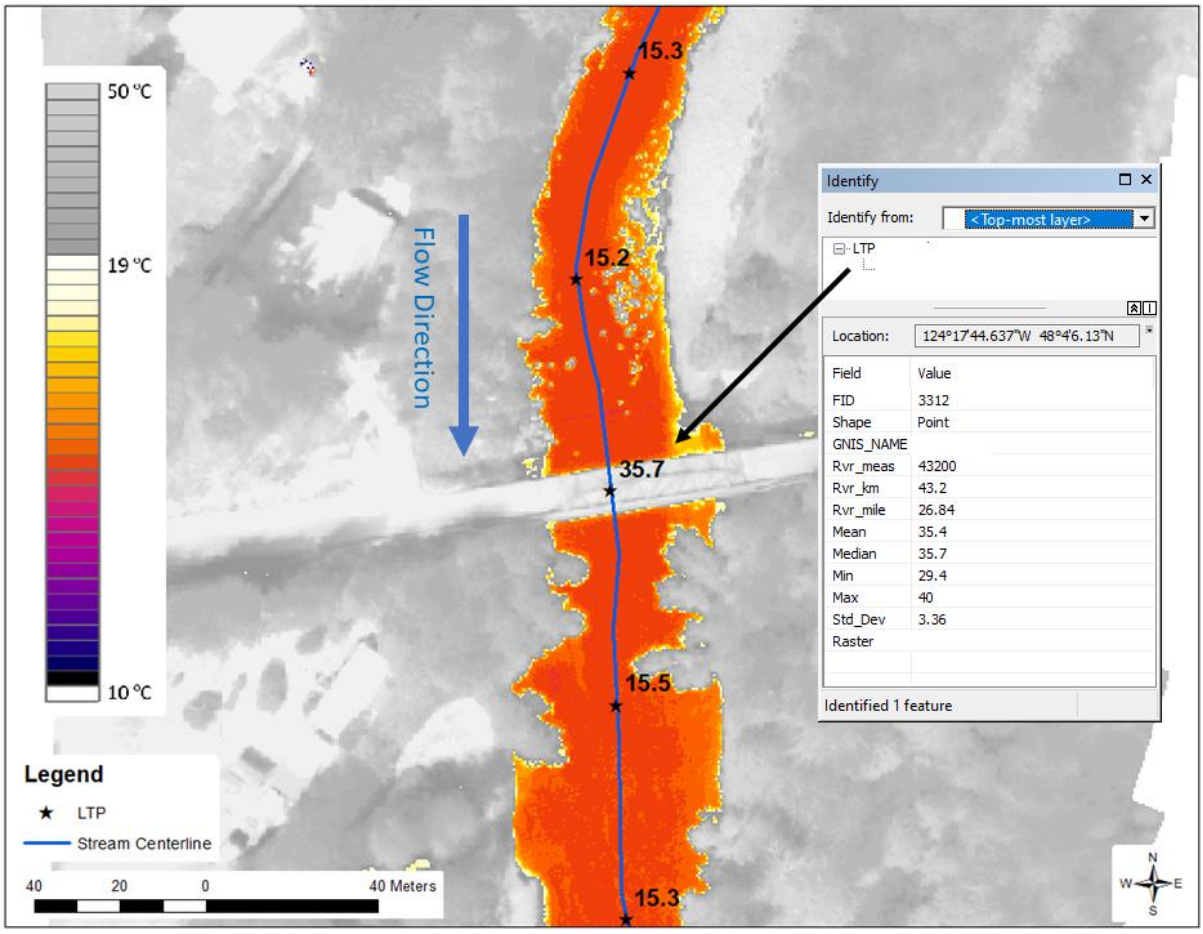

Figure 8: TIR image shows an example of one LTP sampling point that fell on a bridge crossing the river. This point, for an example, can be excluded from the final LTP data by the user.

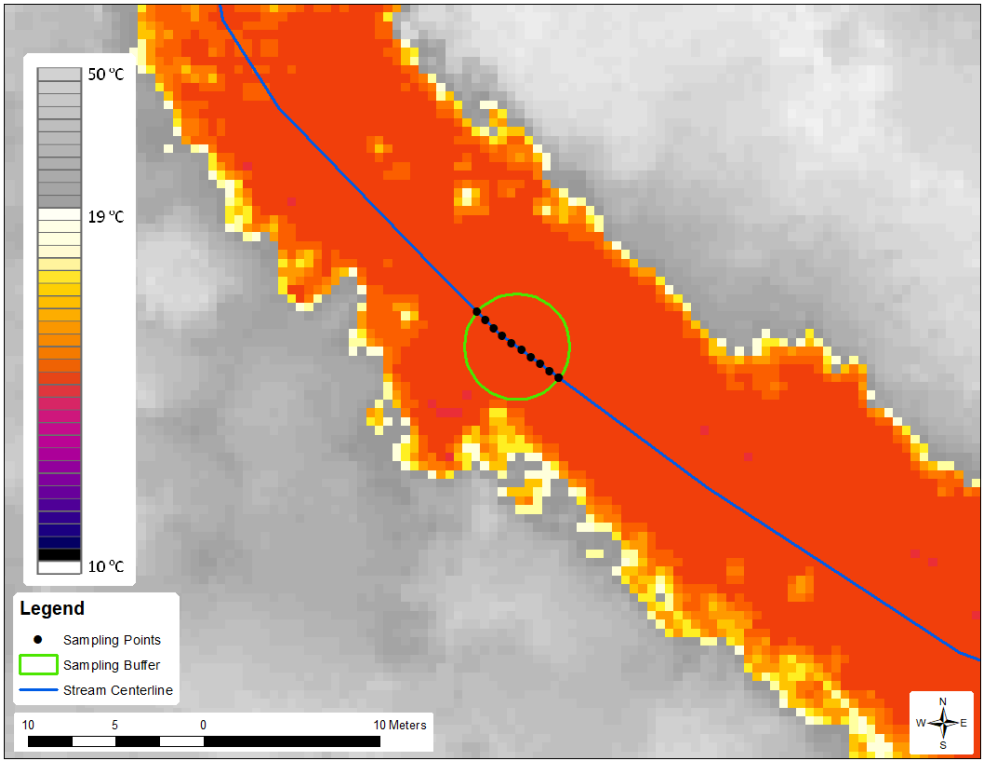

Figure 9: TIR image shows an example of sampling points along the centerline within the predefined buffer.

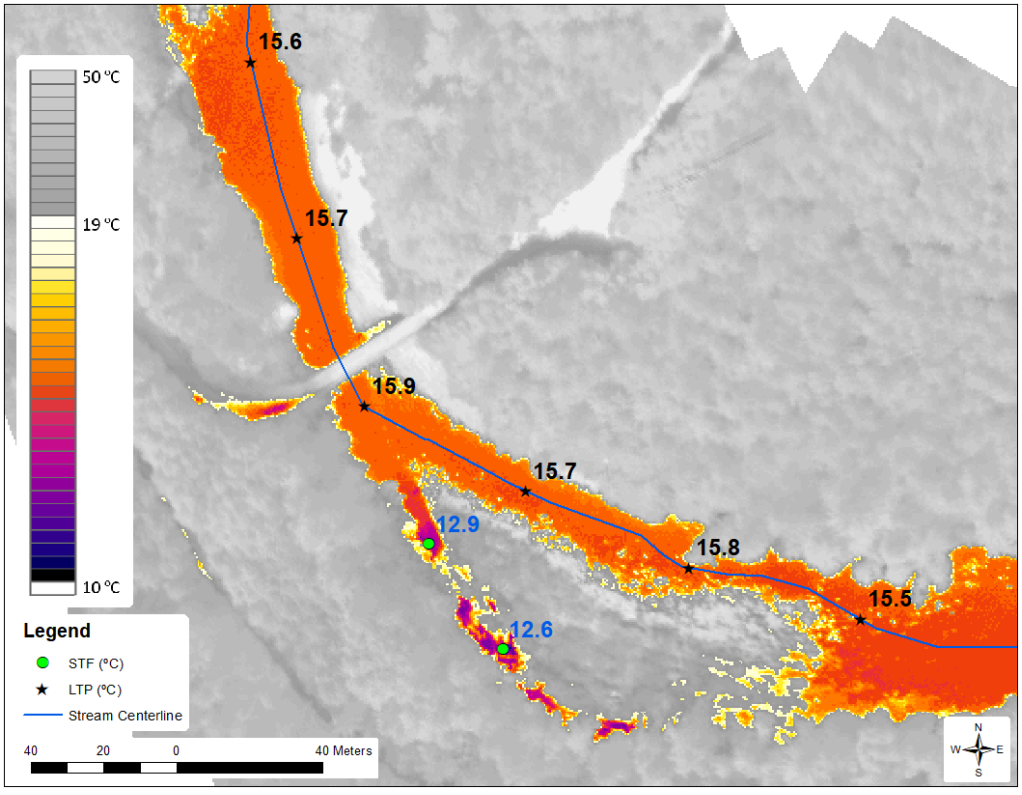

Figure 10: An examples of significant thermal features (STFs) that identify a potential inflow from a side channel or cold-water spring flowing into the main channel.

Table 8: Summary of the processing and analyses steps used in the thermal analysis

Analysis Step	Data File	Description	Software used
Calibrate the thermal imagery	*<STREAM >.tif*	Convert raw TIR image digital number to radiance temperatures based on the sensor's factory calibration. Adjust radiant temperatures based on the ground control kinetic temperatures.	FLIR ResearchIR v. 4.4
Develop color ramp	*<SPAN>.lyr*	Develop color ramps that highlights spatial variability of stream temperatures.	ArcMap v. 10.8
Digitize stream centerlines along main flow path seen in TIR imagery	*Centerline_ <STREAM>.shp*	Digitize the centerlines of the stream based on the final thermal mosaics to best represent the main flow path (AKA the thalweg).	ArcMap v. 10.8
Generate longitudinal temperature profiles (LTP)	*LTP_<STREAM>.shp*	Using automated NV5 tools, a GIS point layer was generated from the stream center line layer at 100-feet intervals. Each point was assigned a river measure and the TIR radiant temperature was sampled based on an average of 5-feet sample buffer radiating out from the center point along the centerline. Low order tributaries were sampled at 10-ft intervals and water temperature summary along the centerline within 3-ft buffer.	ArcMap v. 10.8 NV5 script
Generate significant thermal features (STF)	*STF_<STREAM>.shp*	Digitize points and sample the mosaic for temperature statistical information of potential hyporheic flow, side channels, springs, and urban flow. All mosaic's pixels inside a circular 2-ft buffer were used to summarize water temperature statistics. Each STF is referenced by its distance from the centerline and river mile.	ArcMap v. 10.8 NV5 script
Tabular format and Plots: Longitudinal profiles plots Significant thermal features	*LTP_STF_<STREAM>.xlsx*	Plot temperature against river measure for the longitudinal temperature profile and the manually identified significant features.	Excel

Thermal Infrared Data Processing

The TIR analysis focused on utilizing the thermal signatures to identify features that were relevant to the project objectives. The analysis provides a review of the longitudinal thermal gradient of the stream, significant features at the edge of the stream channel, and point source and non-point source inflows (e.g., tributaries, side channels, groundwater upwelling, seepage, effluents, springs, and hyporheic flow) in the floodplain. The analysis was based on sampling the TIR mosaic along the centerline to generate the longitudinal temperature profile (LTP) and the significant thermal feature (STF) across the floodplain. The results were visualized by plotting the median stream temperature from the LTP and the STF against the stream's length.

The LTP is an informative tool to detect stream temperature gradients and the response to various water inflow sources. It is common to plot the median water temperature against river length, though the other calculated statistical information (especially the mean, maximum, or minimum) can be used as well. The final LTP data excludes most of the non-water features that were accidentally sampled by the automated algorithm. An easy approach to exclude non-water features is by excluding results of high standard deviation and minimum/maximum temperatures. However, further refinement might be required by the end user based on local information and familiarity with the survey area.

Accuracy Assessment Results

TIR imagery was calibrated using the water temperature recorded by in-stream data loggers. The accuracy assessment, a comparison between the water temperatures recorded by the in-stream data loggers and the radiant temperatures derived from the TIR mosaic, is summarized in Table 9. The final mosaic is considered within the specified accuracy requirements when the differences between sampled TIR mosaic mean temperatures (radiant) and the recorded water temperatures is ≤1.0 °C. The accuracy assessment is based on the data recorded by all data loggers within a single river section or mosaic. For this project, the TIR mosaics were within this accuracy threshold.

Table 9: Summary of accuracy assessment values.

AOI	Serial No.	Recorded Water Temperature (°C)	Sampled TIR Mosaic Mean Temperature (°C)	Error (°C)
Whychus Creek	21434366	17.8	17.9	0.1
Indian Ford Creek	21434369	17.7	18.3	0.6
Deer Creek	21434368	17.5	17.7	0.2
McKenzie River	21434376	12.8	12.9	0.1
McKenzie River	21434371	13.2	13.3	0.1
North Fork Siuslaw River	21434370	18.6	18.6	0.0
Fivemile Creek	21434373	16.9	16.9	0.0

North Fork Siuslaw River, McLeod Creek

An area of 164.4 acres and a combined 2.8 km of North Fork Siuslaw River and McLeod Creek were mapped on September 4th (Table 10 and Figure 11). The longitudinal temperature profile (LTP) of NF Siuslaw showed a gradient of downstream warming where the water temperature increases as the bulk of water flows downstream (Figure 12). Water temperature increased from 18 to 19 °C within less than 1km of distance. But the temperature dropped back to 18 °C due to the inflow from McLeod Creek which was 1.5 °C colder than Siuslaw river at that point (Figure 13). The NF Siuslaw River temperature increased again downstream of the confluence with McLeod Creek.

It was not feasible to generate an LTP plot for McLeod Creek due to the narrow channel and overhanging vegetation.

Table 10: List of surveyed tributaries and their lengths.

Tributary Name	Tributary Length (km)
NF Siuslaw River	1.82
McLeod Creek	0.97

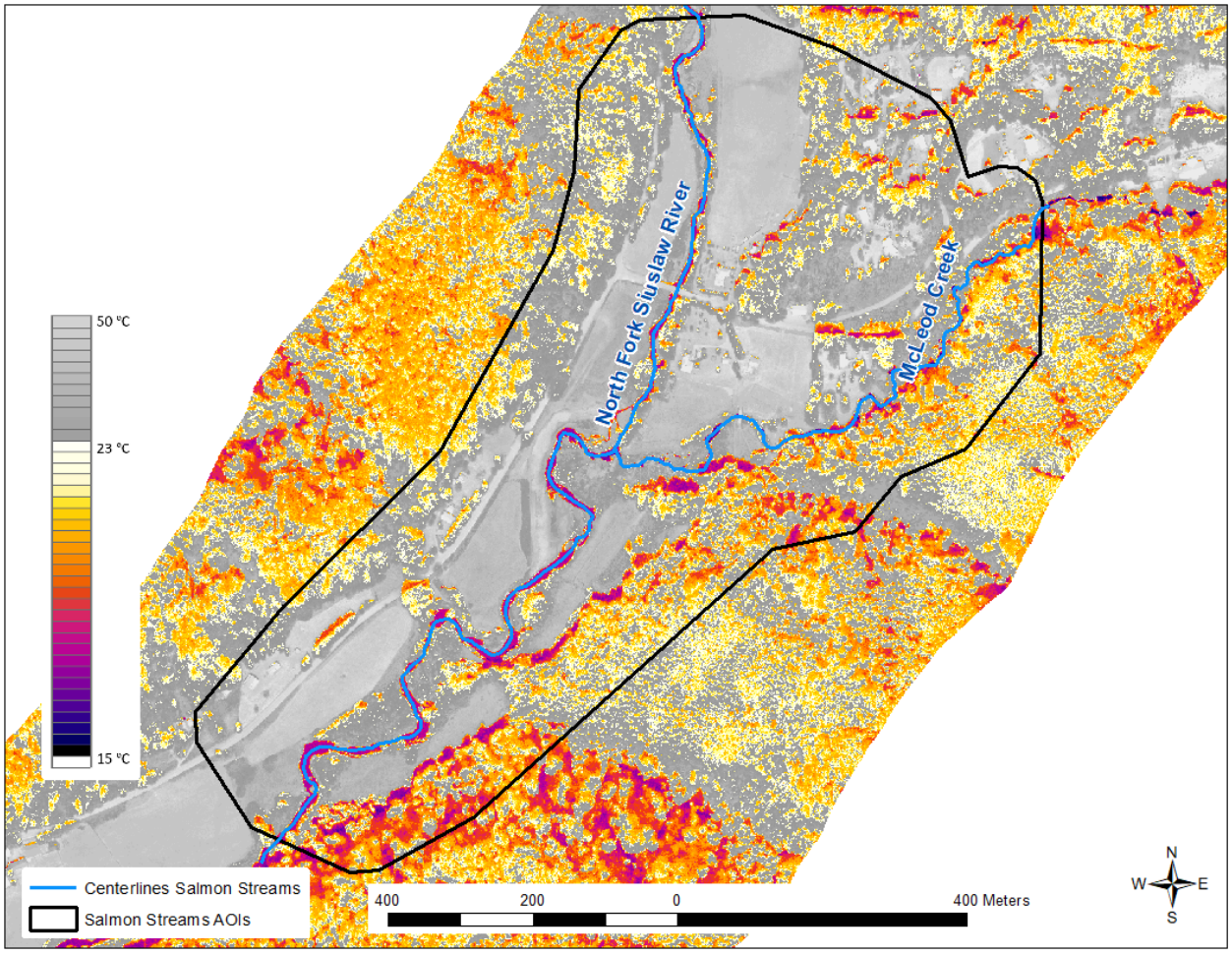

Figure 11: NF Siuslaw River and McLeod Creek survey area.

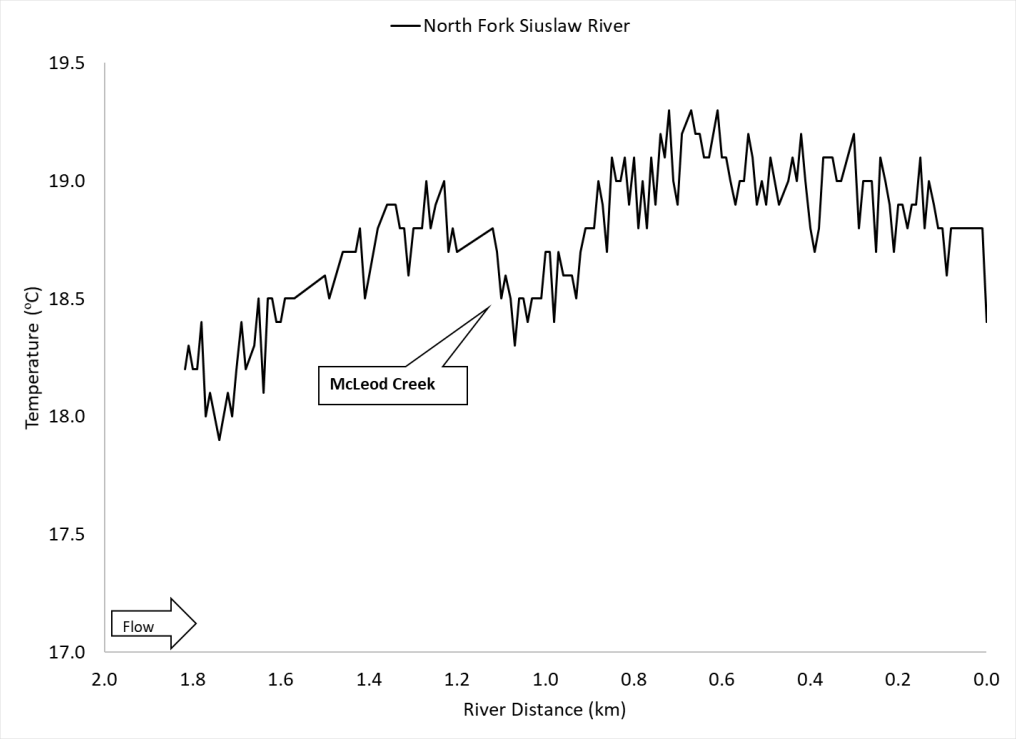

Figure 12: LTP of NF Siuslaw River showing the downstream warming and cooling gradients. The plot shows median water temperature (°C).

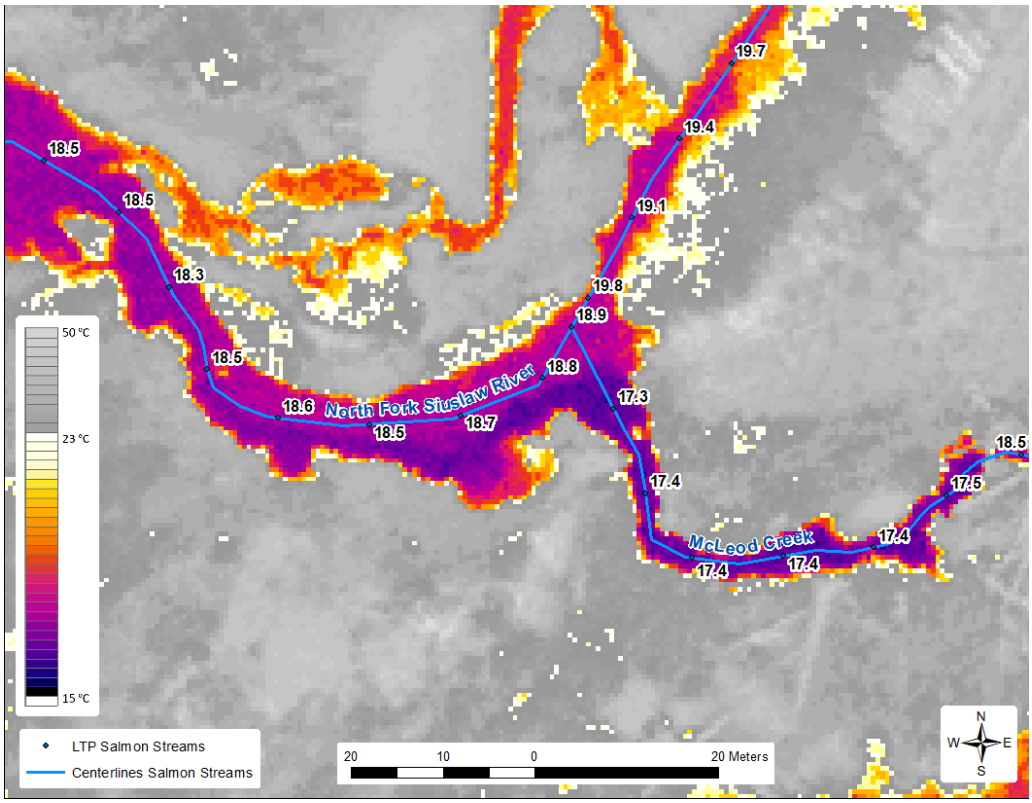

Figure 13: The confluence of McLeod Creek with NF Siuslaw River showing the latter was 1.5 °C warmer.

McKenzie River, Quartz Creek, Cone Creek, Ennis Creek

A total of 8.1 km of the McKenzie River main section were mapped on September 4th to which three creeks flow in: Cone Creek, Quartz Creek, and Ennis Creek (Table 11, Figure 14). The LTP plot shows a downstream warming gradient along the upstream section (river km 8 to 4.8) where the water temperature increases from 12.6 to 13.3 °C (Figure 15). Both Quartz Creek and Ennis Creek flow directly into the main channel of the McKenzie River at roughly 7 °C warmer than the main channel (Figure 16 and Figure 17). However, their low discharge, relative to the main channel, don't have a significant impact on the water temperature (Figure 15). Cone Creek flew into a side channel of the McKenzie River at a low flow that made it difficult to generate LTP plot or analysis.

Table 11 List of surveyed tributaries and their lengths.

Tributary Name	Tributary Length (km)
McKenzie River	8.1
Quartz Creek	3.4
Cone Creek	0.6
Ennis Creek	0.9

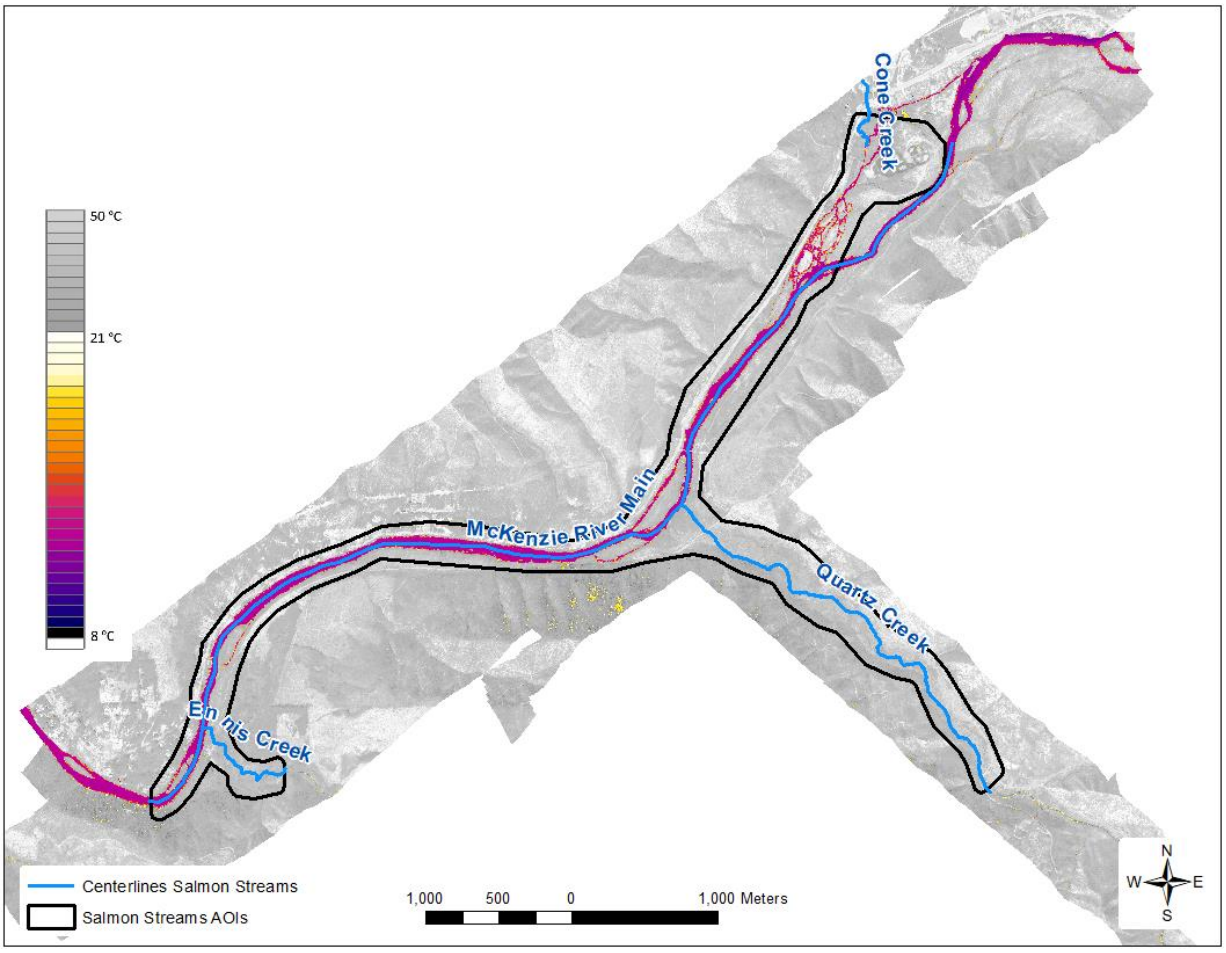

Figure 14: McKenzie River survey area (main section).

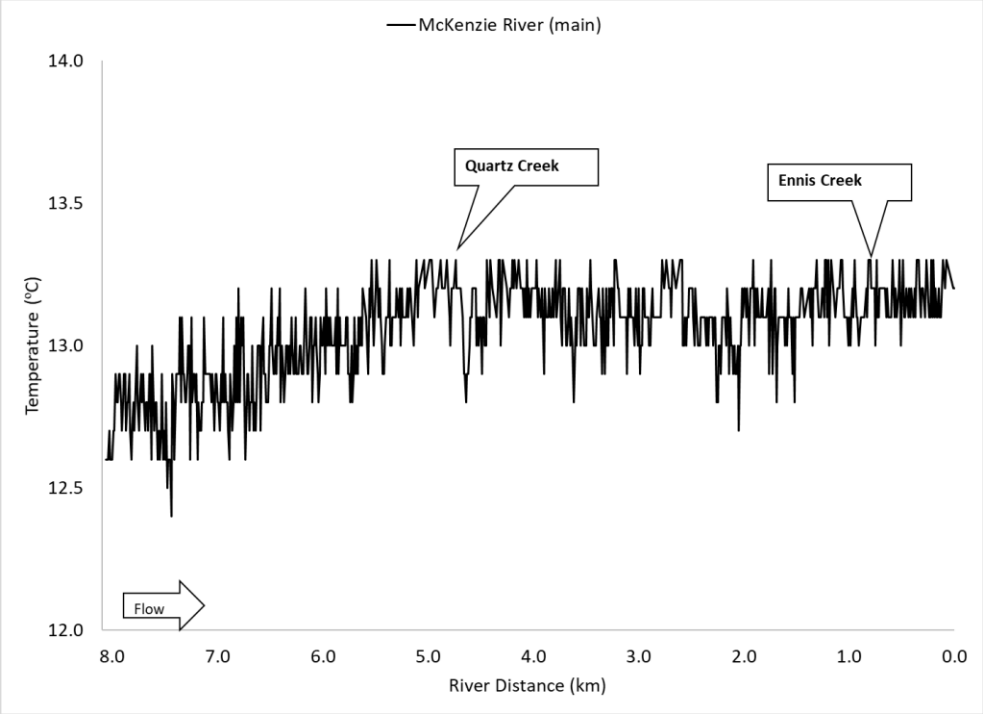

Figure 15: LTP of the McKenzie River showing the downstream warming gradient (12.6 to 13.3°C) between river km 8 and 4.8 where Quartz Creek flows in. The river water temperature stabilized for the rest of the surveyed section. The plot shows median water temperature (°C).

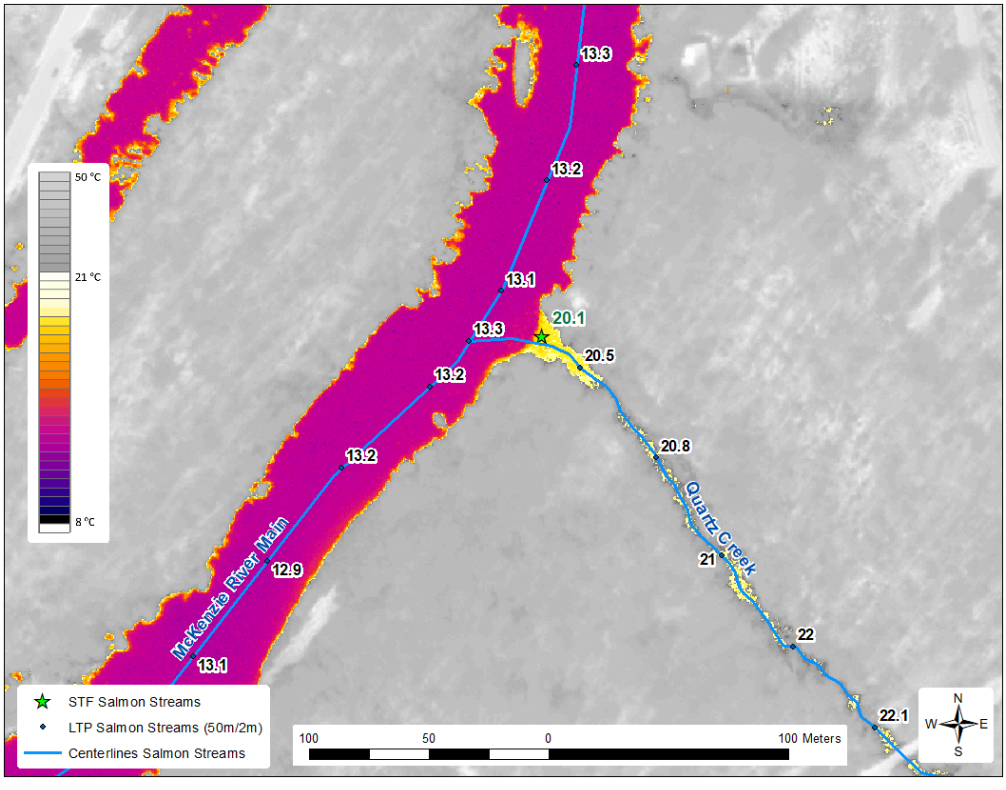

Figure 16: The confluence of Quartz Creek with the McKenzie River showing temperature difference of nearly 7 °C.

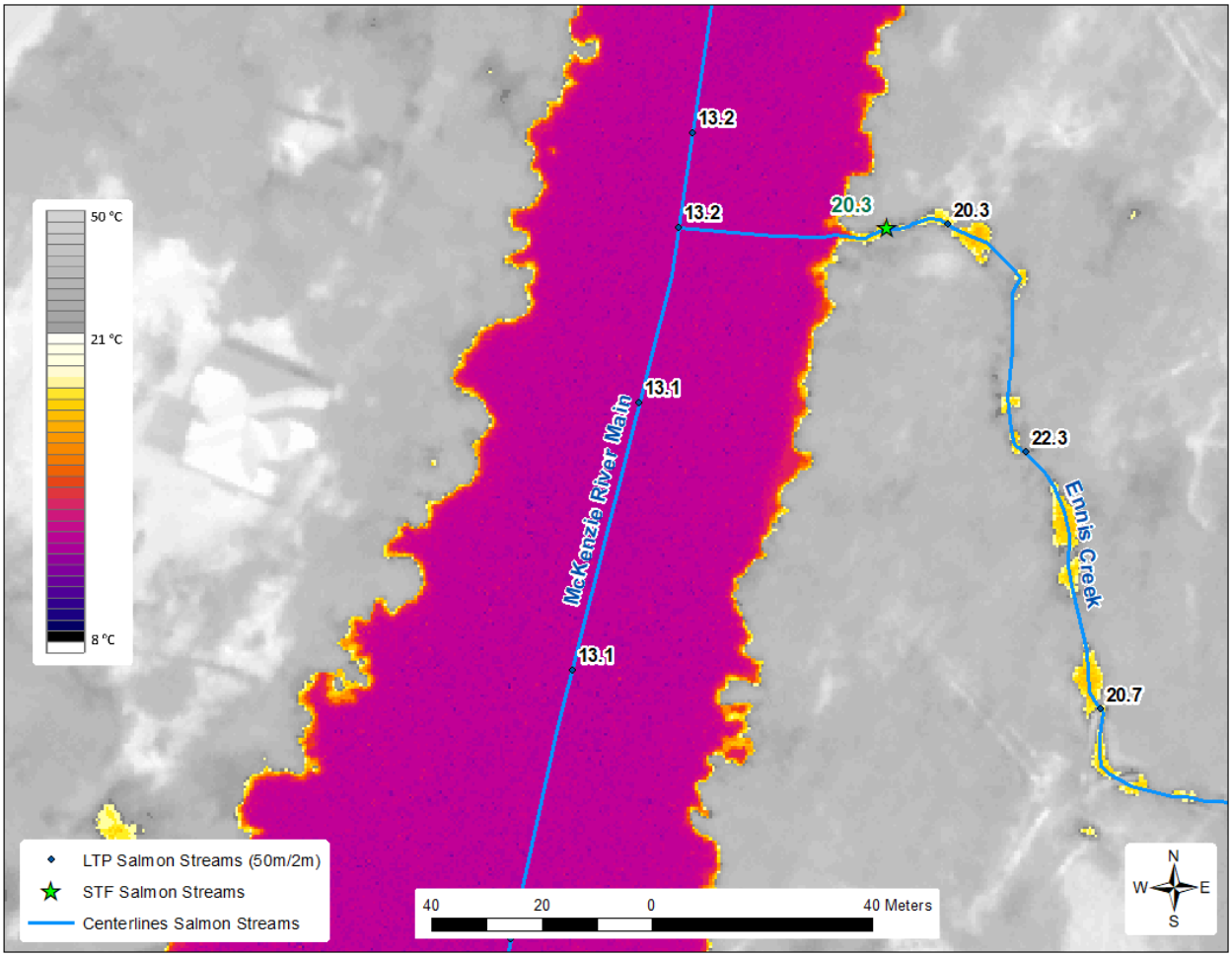

Figure 17: The confluence of Ennis Creek with the McKenzie River showing temperature difference of nearly 7 °C.

South Fork McKenzie River and McKenzie River (Section A)

A total of 2.3 km of the South Fork McKenzie River were mapped on September 4th (Table 12, Figure 18). The LTP plot shows a downstream warming gradient along the SF McKenzie River length where water temperature increased from nearly 14.0 °C to 15.9 °C at the confluence with the mainstem McKenzie River(Figure 19). While the mainstem McKenzie River was running at 12.2 °C, the contribution of the SF McKenzie River warmed up it temperature to nearly 14.0 °C downstream of the mixing zone (Figure 20).

Table 12 List of surveyed tributaries and their lengths.

Tributary Name	Tributary Length (km)
SF McKenzie River	2.3

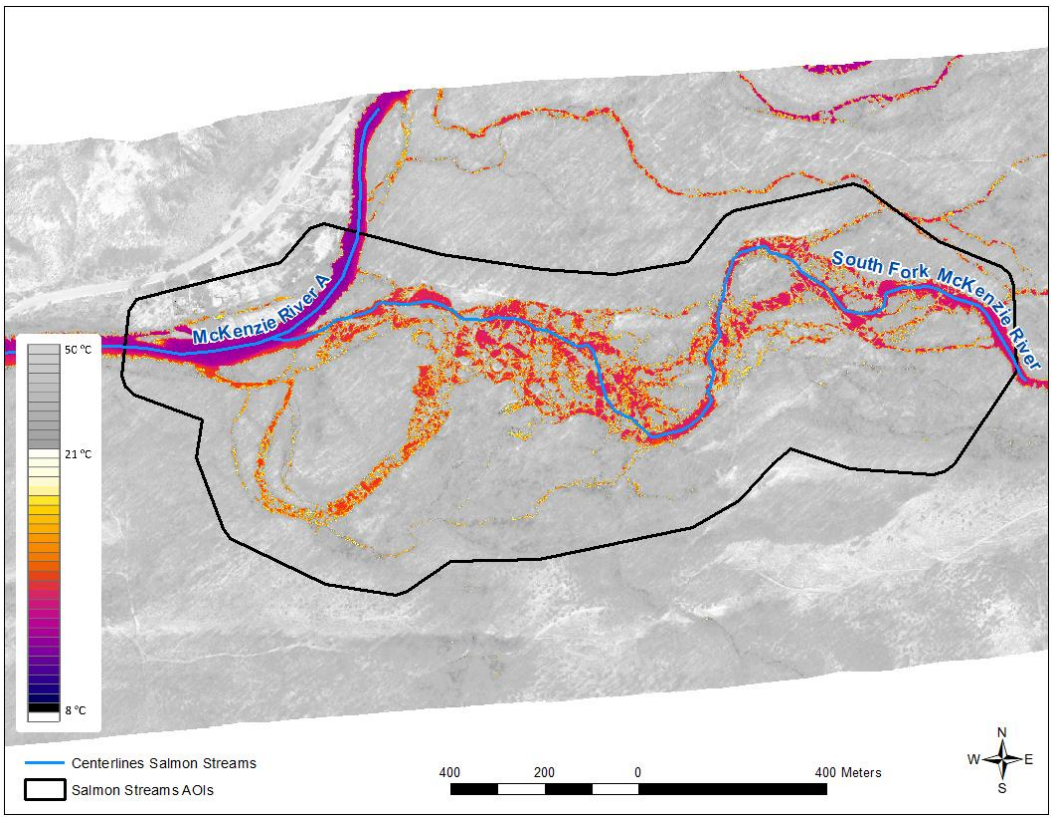

Figure 18: South Fork McKenzie River survey area.

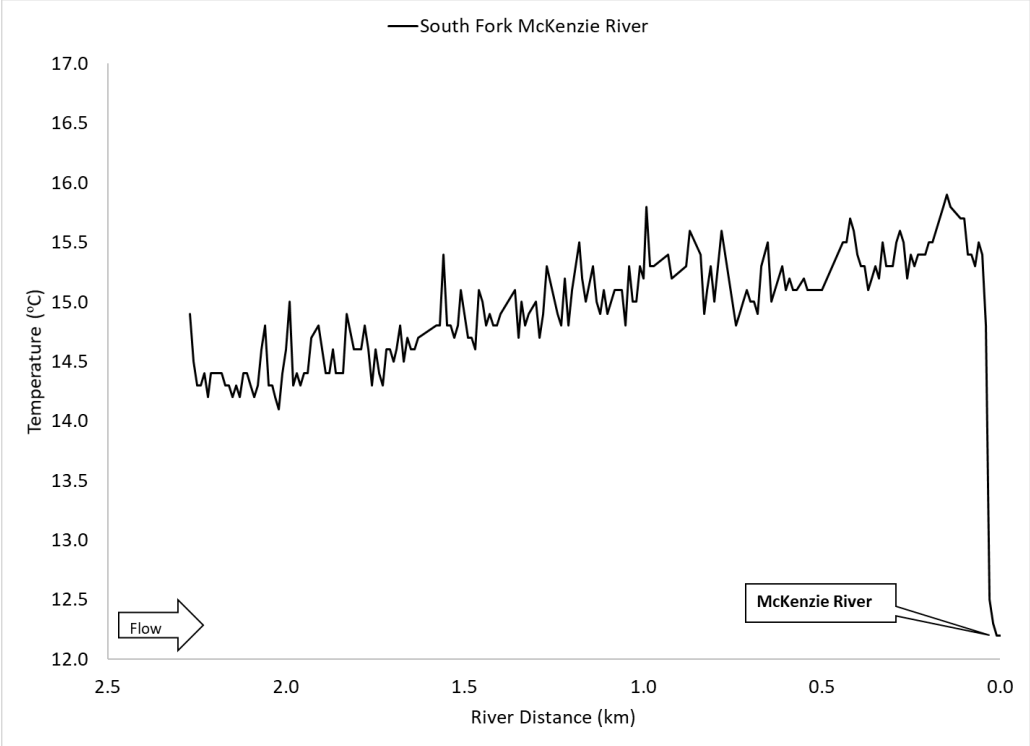

Figure 19: LTP of the SF McKenzie River showing the downstream warming gradient (14.0 to 15.9°C) within 2.3 km of the surveyed area. The plot shows median water temperature (°C).

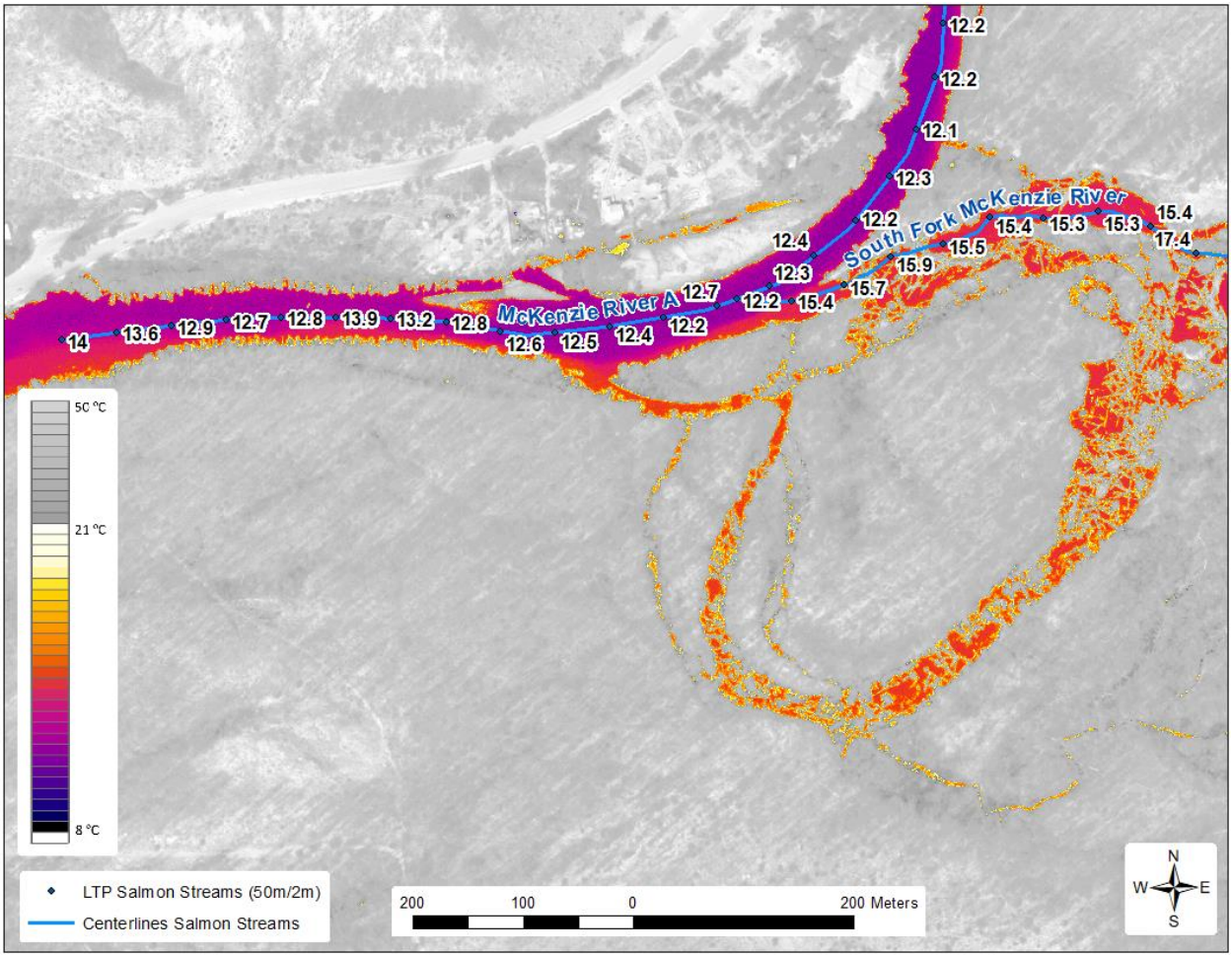

Figure 20: The impact of warm water inflow from the SF McKenzie River into the mainstem McKenzie River causing 1.8 °C warming of the later.

Deer Creek and McKenzie River (Section b)

A total of 3.1 km of the Deer Creek were mapped on September 2nd (Figure 21). Also partial sections of Budworm Creek and mainstem McKenzie River were mapped (Table 13).The LTP plot shows a downstream warming gradient along Deer Creek's short path, from 14 °C to nearly 20 °C (Figure 22). The warm water inflow from Deer creek caused a slight warming to the McKenzie River, from 10.0 °C to 10.7 °C (Figure 23).

There may be several potential factor to cause the rapid downstream warming. Despite the complexity of the channel and the presence of large tree logs, a combination of high-water residence-time and conditions of minimal or no riparian vegetation could have resulted in high solar radiation input throughout the daytime. Furthermore, the shallow active channel (mean high ratio of surface water to water volume/discharge) may have accelerated the solar heating effect. There were no signs of cold-water inflow (such as seeps, springs, or hyporheic exchange zones) present along the channel of Deer Creek.

Table 13 List of surveyed tributaries and their lengths.

Tributary Name	Tributary Length (km)
SF McKenzie River	3.1
Budworm Creek	0.5
McKenzie River	0.4

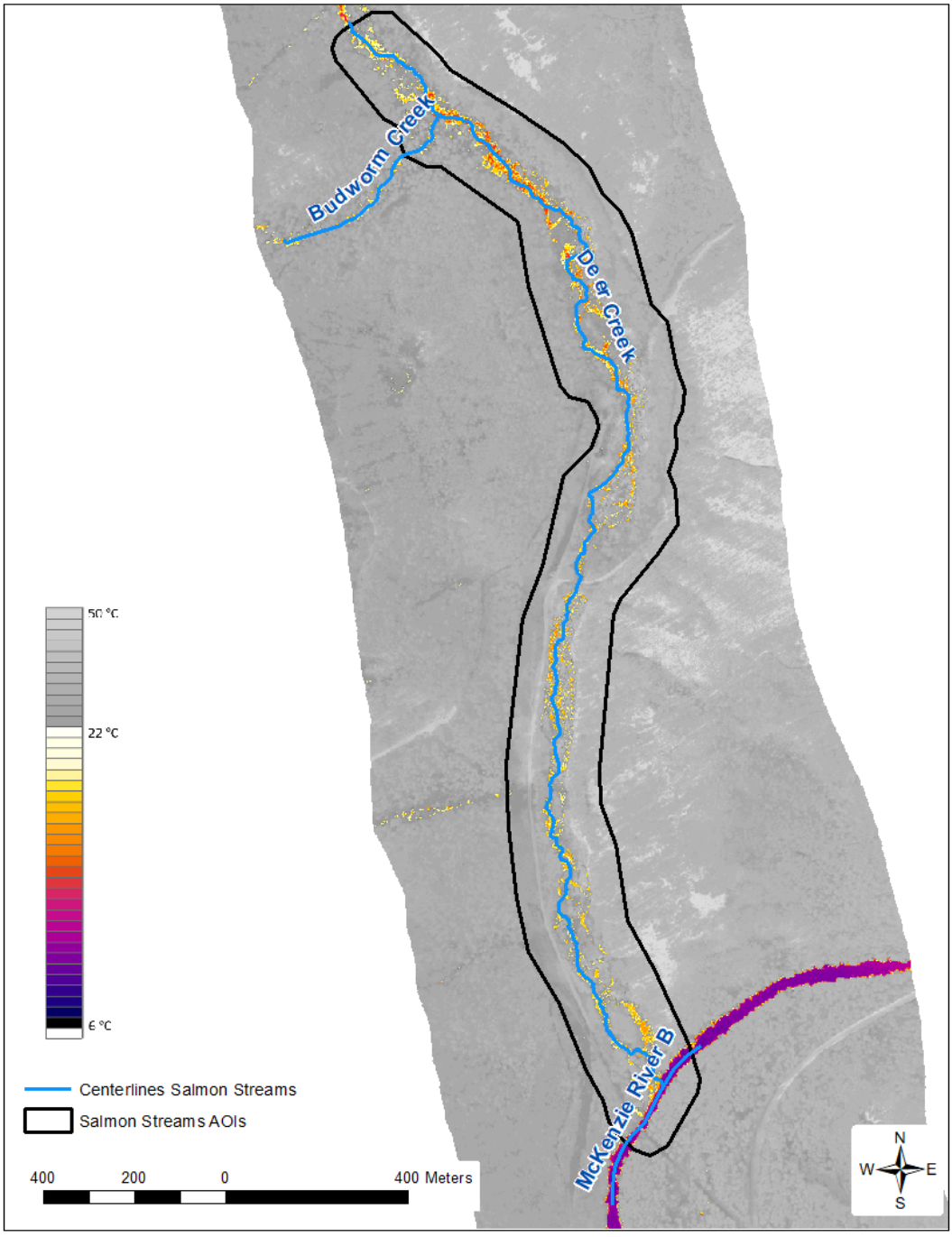

Figure 21: Deer Creek survey area.

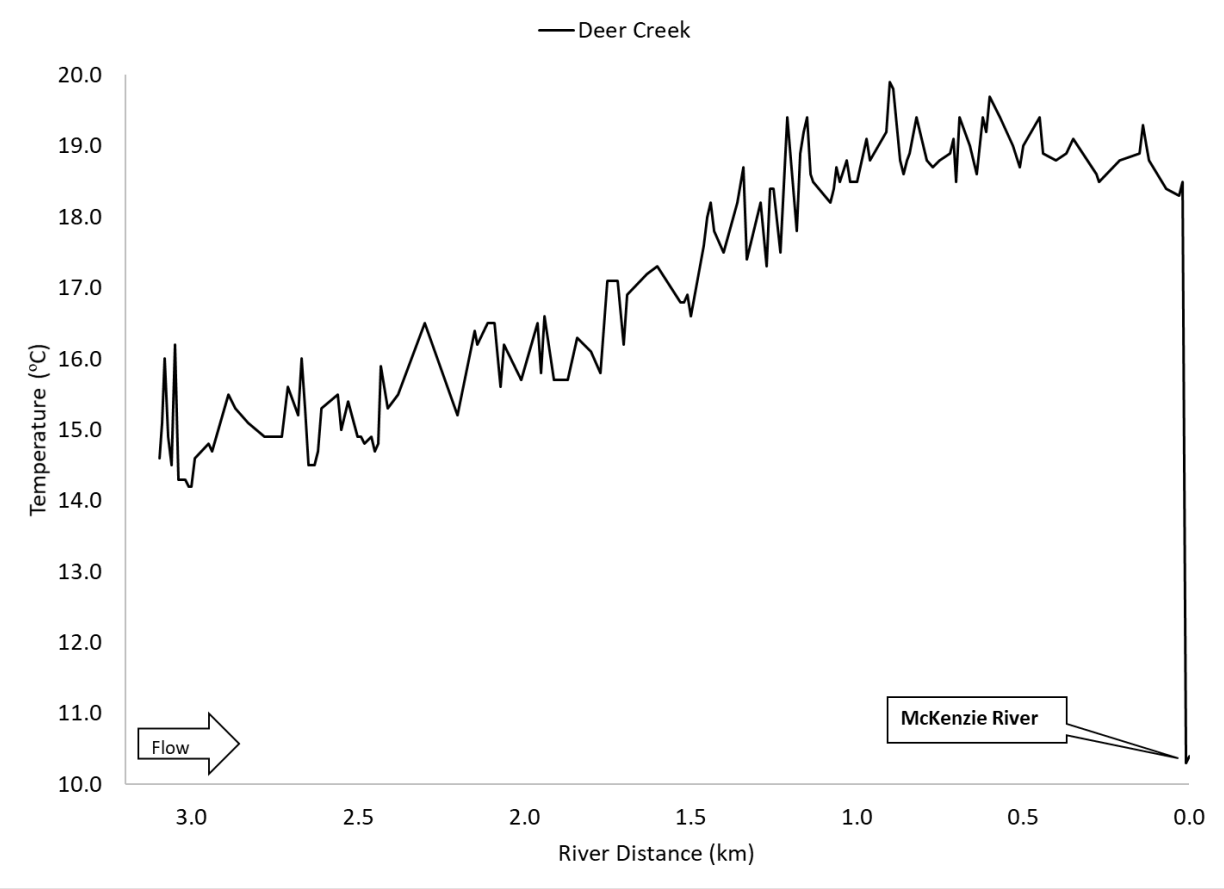

Figure 22: LTP of Deer Creek showing the stead downstream warming gradient along its 3.1 km channel length. Water temperature increased from 14 °C to nearly 20 °C by the time it flowed into the McKenzie River. The warm water inflow from Deer creek cause a slight warming to the McKenzie River from 10.0 °C to 10.7 °C. The plot shows median water temperature (°C).

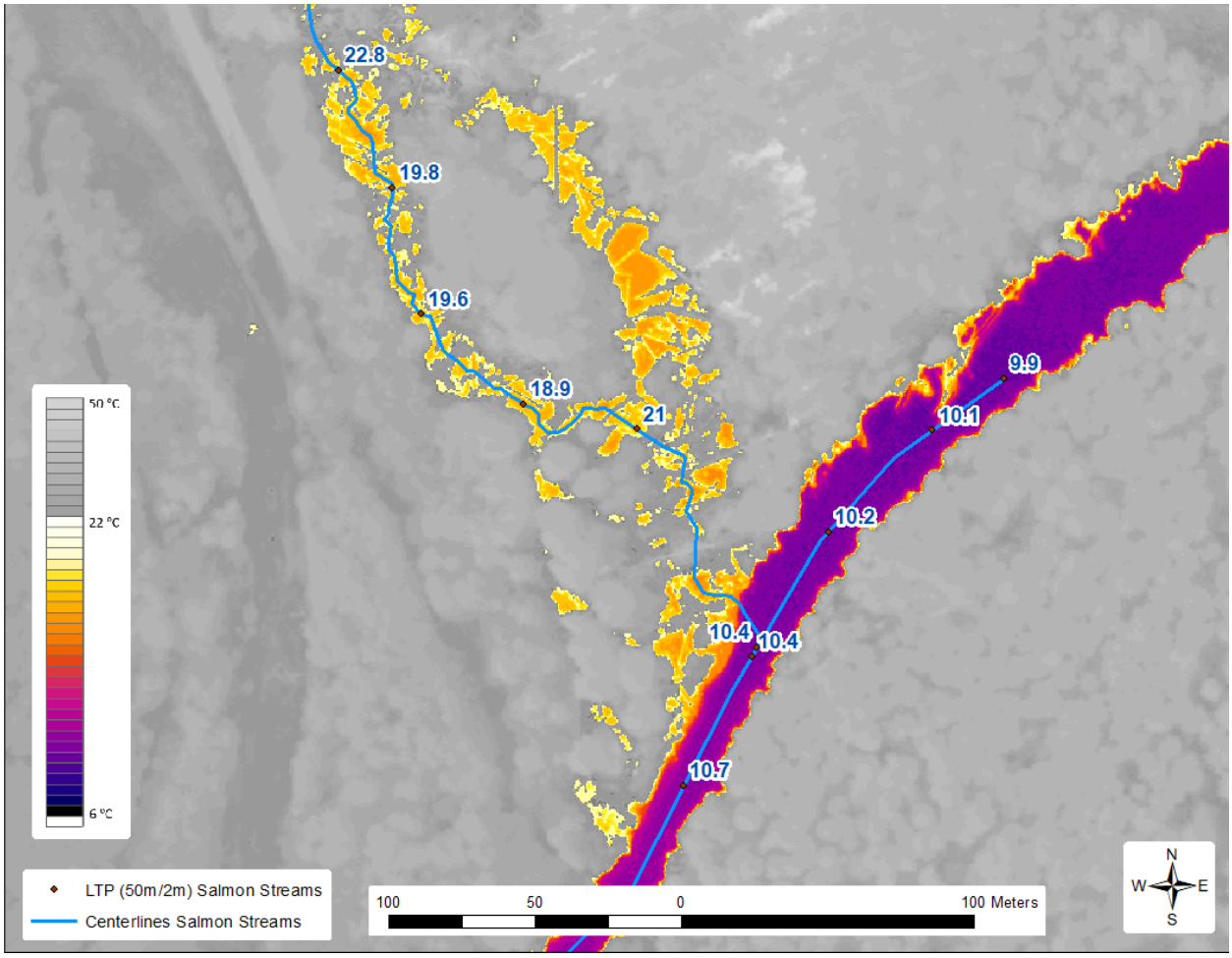

Figure 23: The impact of warm water inflow from Deer Creek into the McKenzie River causing 0.7 °C warming of the later.

Whychus Creek

A total of 6.2 km of Whychus Creek were mapped on September 2nd (Table 14, Figure 24) showing a downstream warming gradient along river section 6.2 to 2. Water temperature increased from below 18 °C to over 21 °C. Water temperature along the lower 2 km of the surveyed section remained relatively steady between 21 and 22 °C. The identified significant thermal features had temperatures close to those of the main channel, mostly within 1 °C higher or lower (Figure 26 and Figure 27).

Table 14 List of surveyed tributaries and their lengths.

Tributary Name	Tributary Length (km)
Whychus creek	6.2

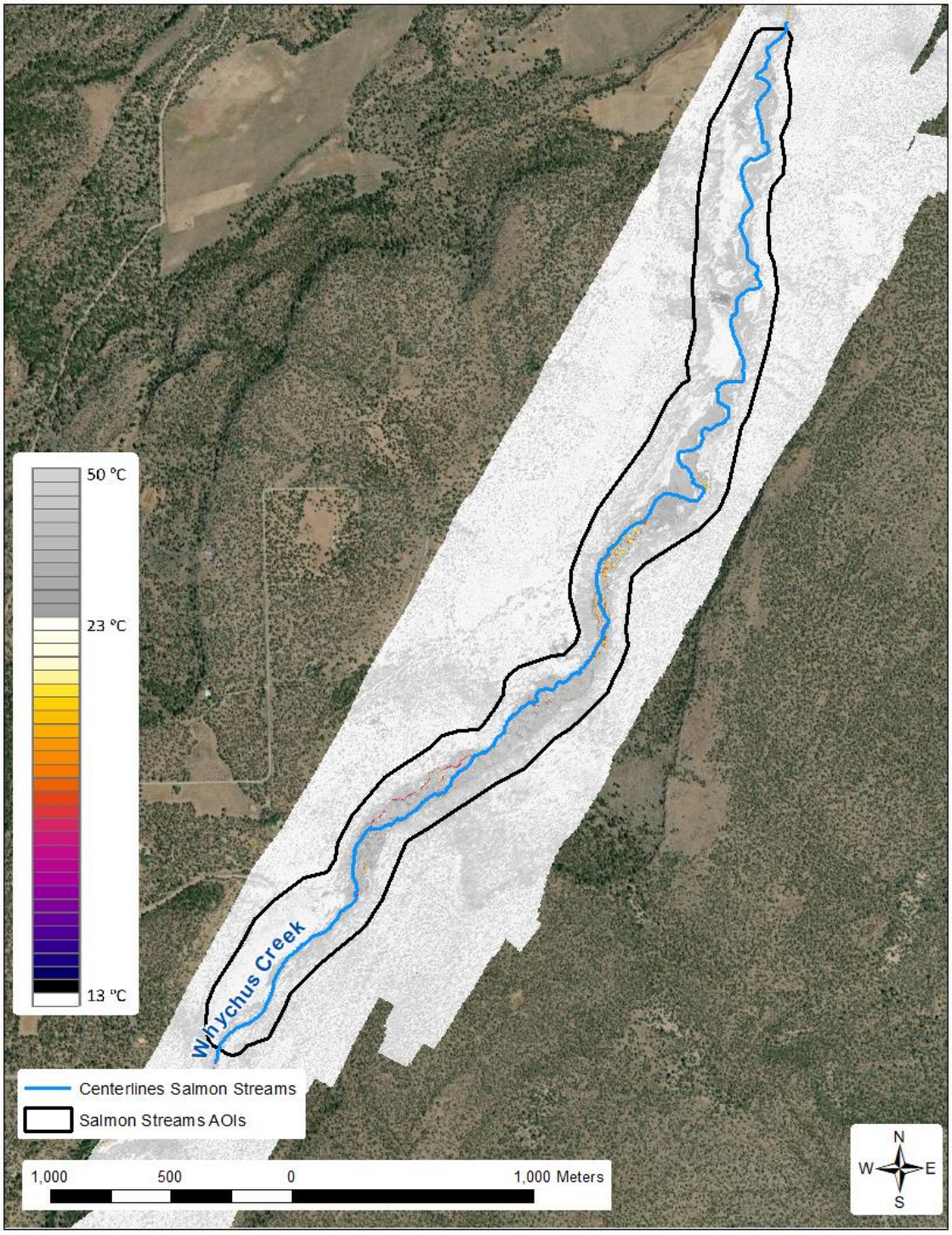

Figure 24: Whychus Creek survey area.

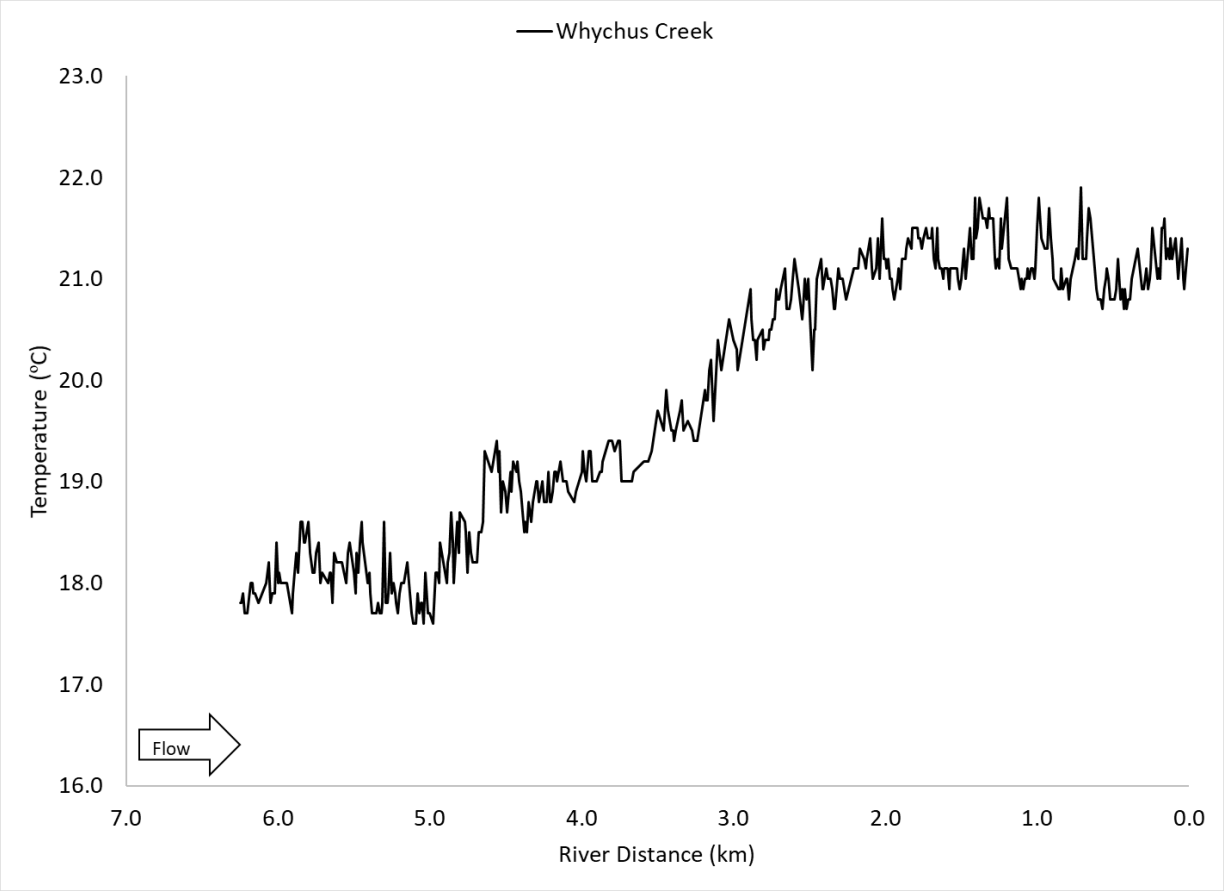

Figure 25: LTP of Whychus Creek showing the downstream warming gradient along river section 6.2 to 2. Water temperature increased from lower than 18 °C to over 21 °C. Water temperature along lower 2 km of the surveyed section remained relatively steady between 21 and 22 °C. The plot shows median water temperature (°C).

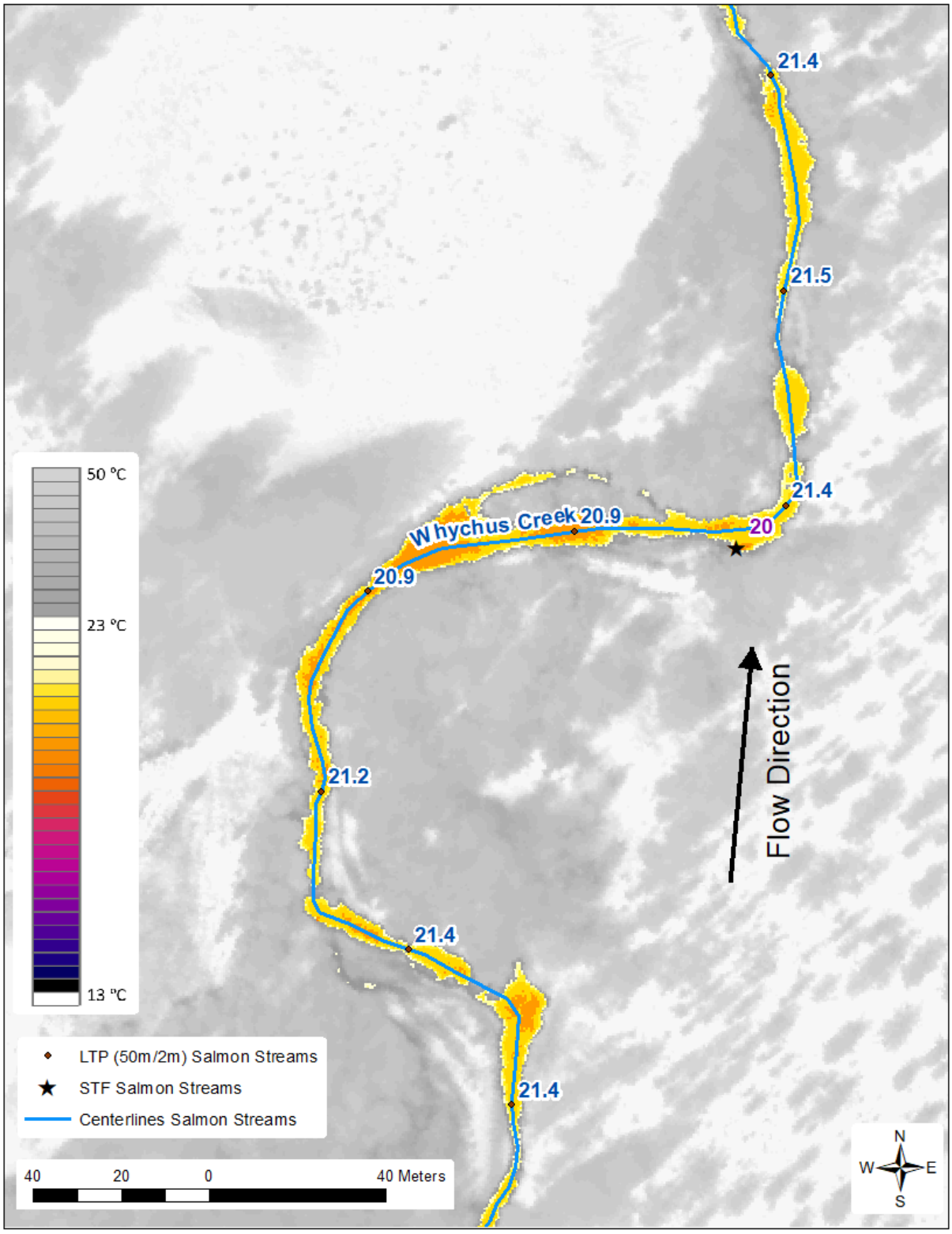

Figure 26: LTP and STF data overlaying TIR data. The identified STF was nearly 1 °C lower than the water in the channel representing a potential hyporheic exchange zone or a small spring.

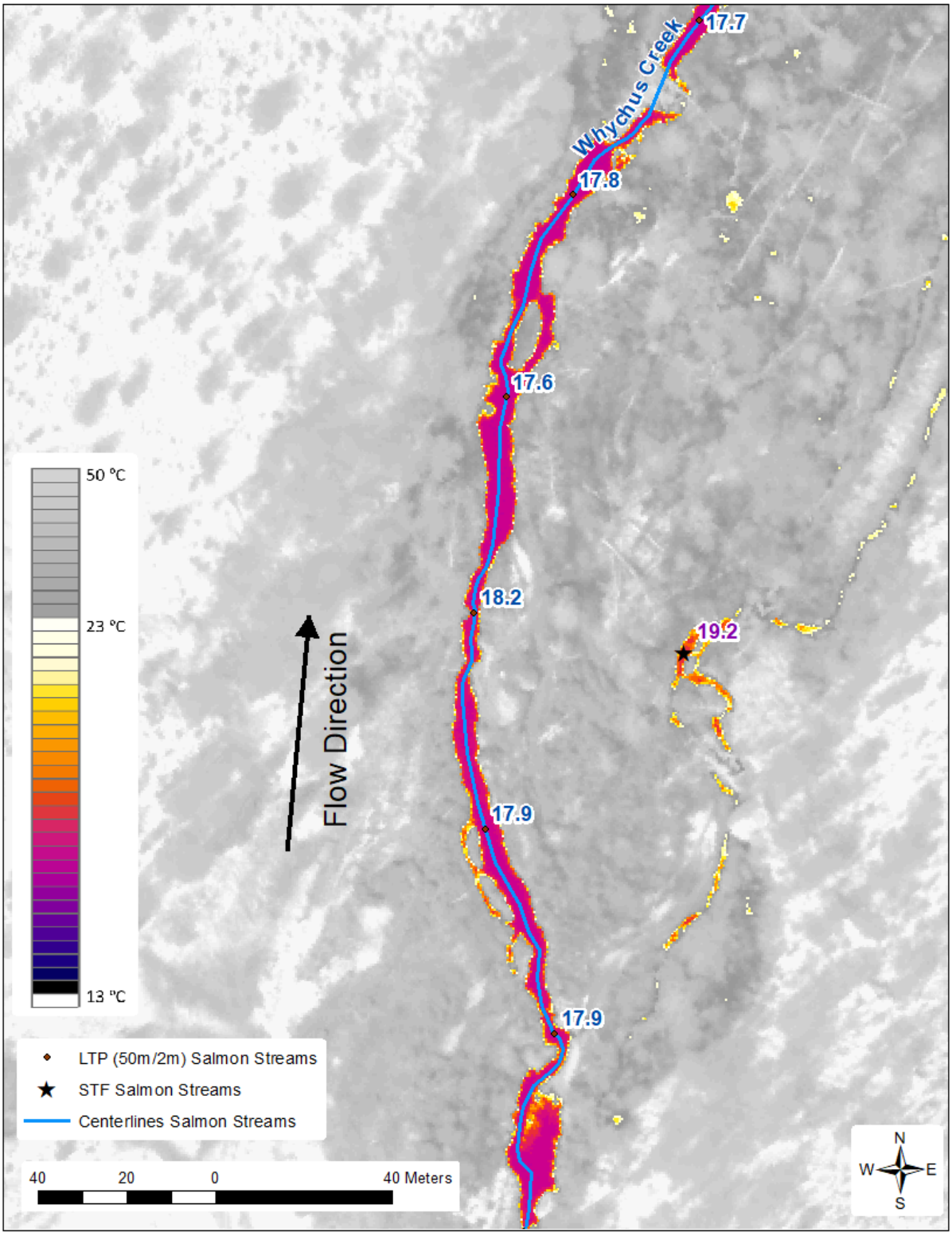

Figure 27: LTP and STF data overlaying TIR data. The identified STF of the side channel was nearly 1 °C warmer than the water in the channel.

Indian Ford Creek

A total of 6.1 km of Indian Ford Creek were mapped on September 2nd (Table 15, Figure 24). The survey data shows the headwaters of Indian Ford Creek which are springs with temperatures as cold as 5 °C (Figure 29). The creek flows through the aerated ponds at the foothills of Black Butte (Figure 30) which aim to maintain circulation and flow of the waters in the ponds. Water temperature exhibited a downstream warming gradient beginning at 5 °C and reaching 19.3 °C by aerated ponds downstream. Generating the LTP plot was not successful for Indian Ford Creek because of the low flow and narrow channel along the section of river km 3.6 to 0. The upstream section of river km 6.1 to 3.6 was characterized by a series of ponds connected by narrow channels that were hard to sample using the TIR data. Nevertheless, water in the ponds along the channel exhibited a wide range of temperatures which are shown in the LTP's plot (Figure 31).

Table 15 List of surveyed tributaries and their lengths.

Tributary Name	Tributary Length (km)
Indian Ford Creek	6.1

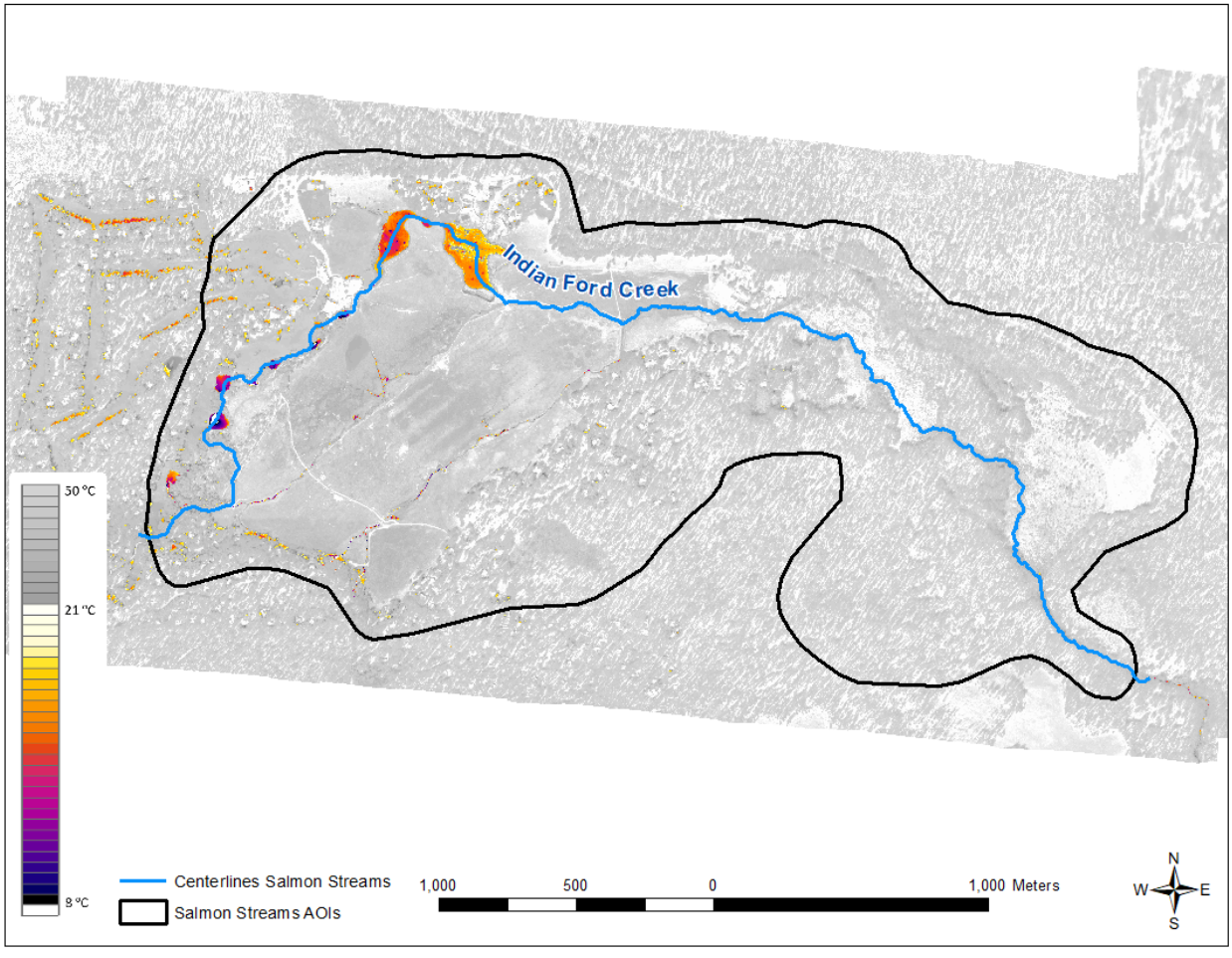

Figure 28: Indian Ford Creek survey area.

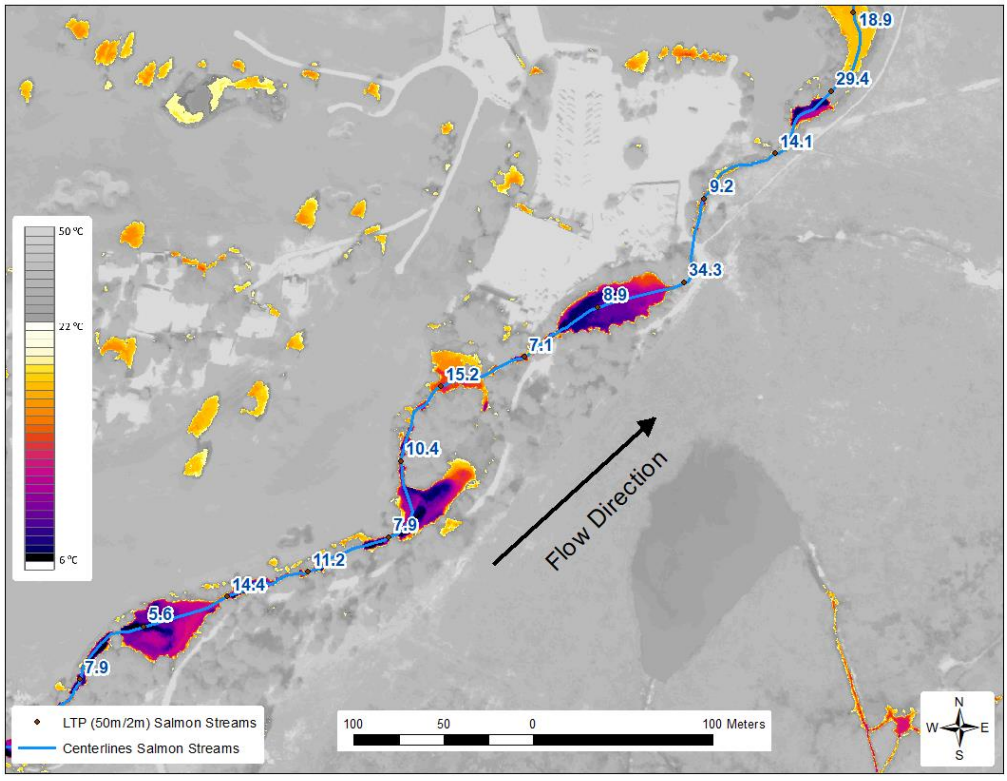

Figure 29: LTP data overlaying TIR data along the headwaters of Indian Creek.

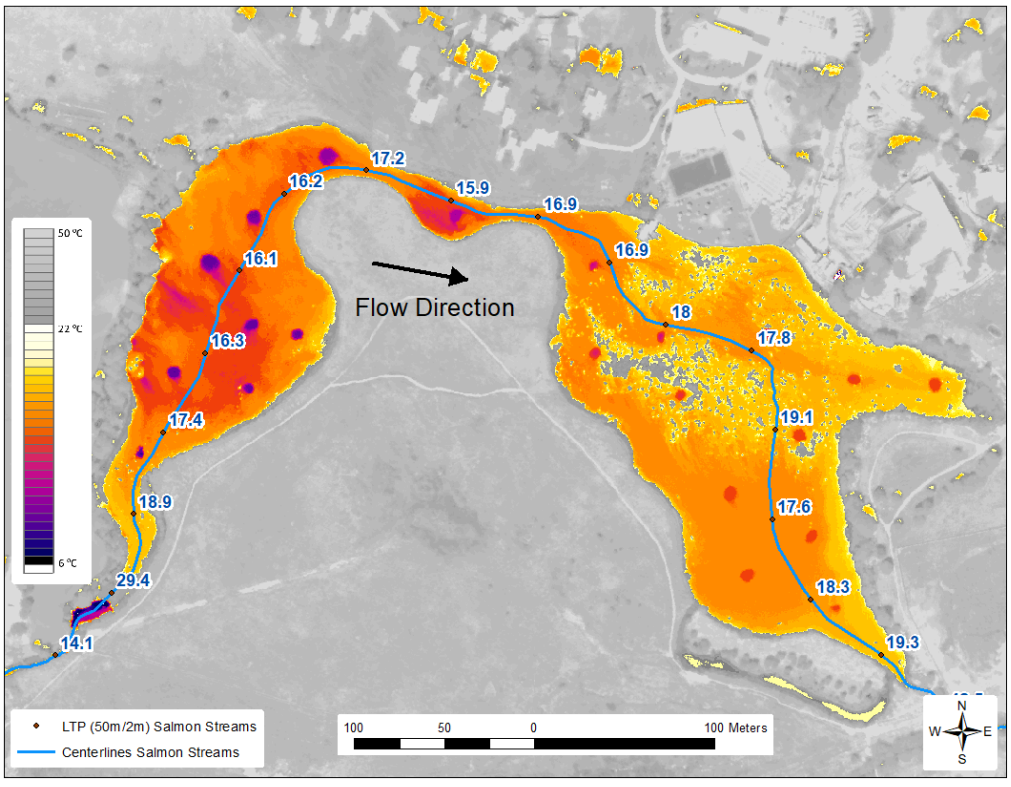

Figure 30: LTP data overlaying TIR data along the aerated ponds.

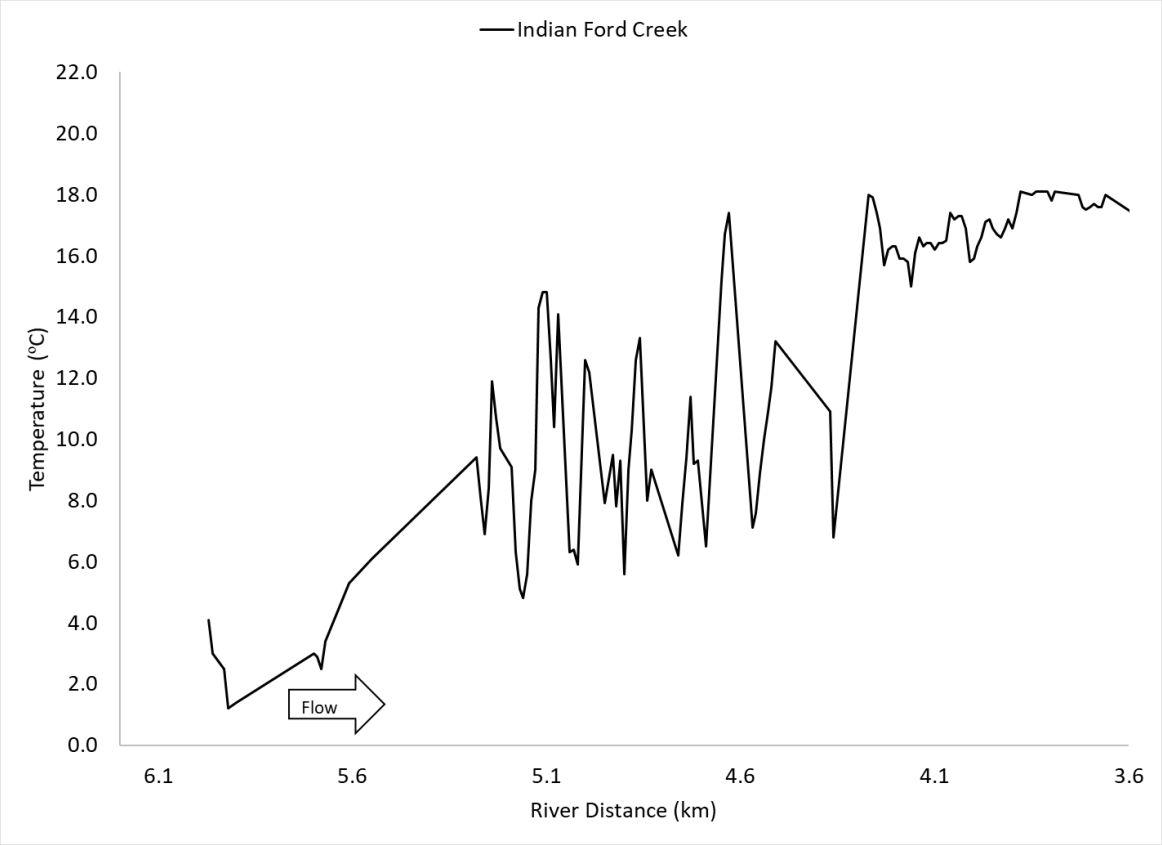

Figure 31: LTP of Indian Ford Creek showing the downstream warming gradient along river section 6.1 to 3.6. The fluctuation along the middle section here is a result of the lack of water mixing found in the ponds along the surveyed channel. The section downstream of river km 3.6 was too narrow and had low flow preventing the generation of a proper LTP plot. The plot shows median water temperature (°C).

Fivemile Creek and Bell Creek

A total of 9.0 km of Fivemile Creek and 2.6 Bell Creek were mapped on September 1st (Table 16, Figure 32). For the majority of the surveyed section, the active channel was covered by riparian vegetation and water vegetation which obstructed the thermal sensor's view. This obstruction caused the LTP plot generation to fail for most of the stream length. It is possible, however, to zoom and focus on stream stretches where the water surface was exposed (no overhanging vegetation or water vegetation) to review the thermal data. Such sites appear as cold patches surrounding by warmer banks or vegetation ().

Table 16 List of surveyed tributaries and their lengths.

Tributary Name	Tributary Length (km)
Fivemile Creek	9.0

Bell Creek	2.6

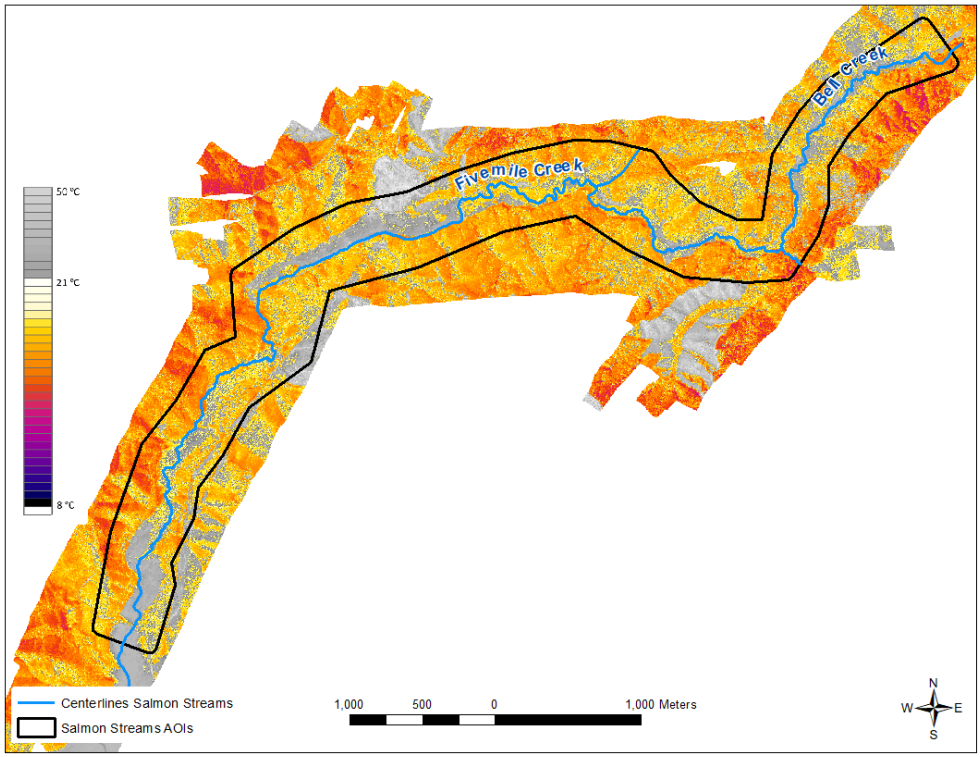

Figure 32: Fivemile Creek and Bell Creek survey area.

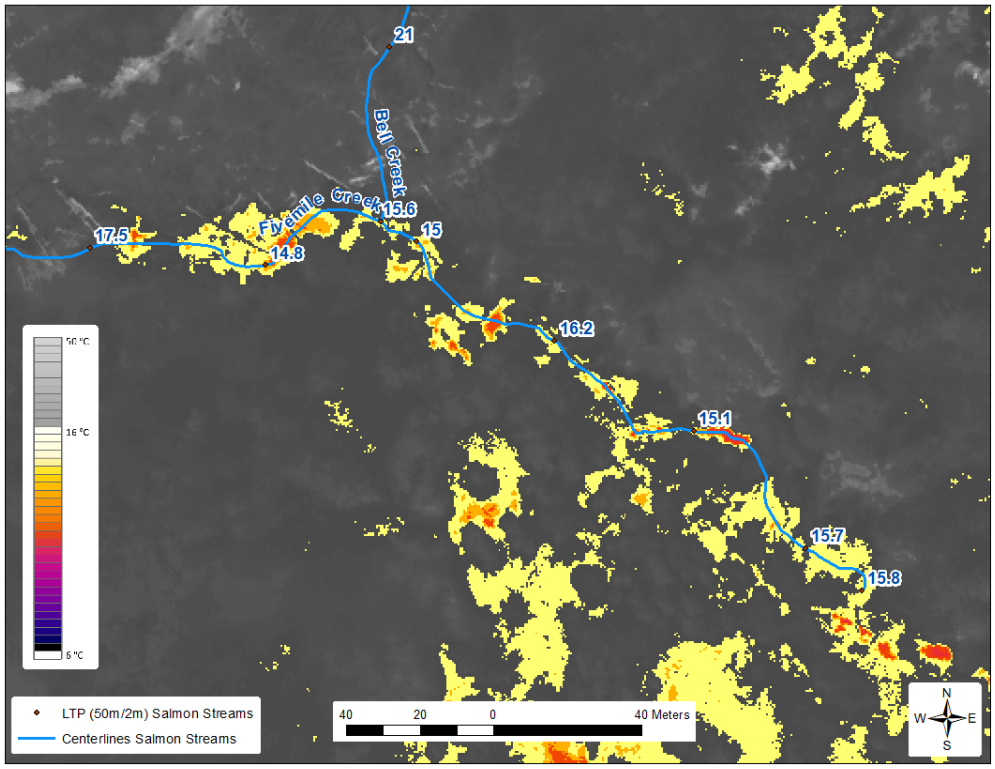

Figure 33: LTP overlayed on top of TIR data showing Bell Creek flowing into Fivemile Creek. This figure shows the patches of exposed water surface along the stream. The plot shows median water temperature (°C).

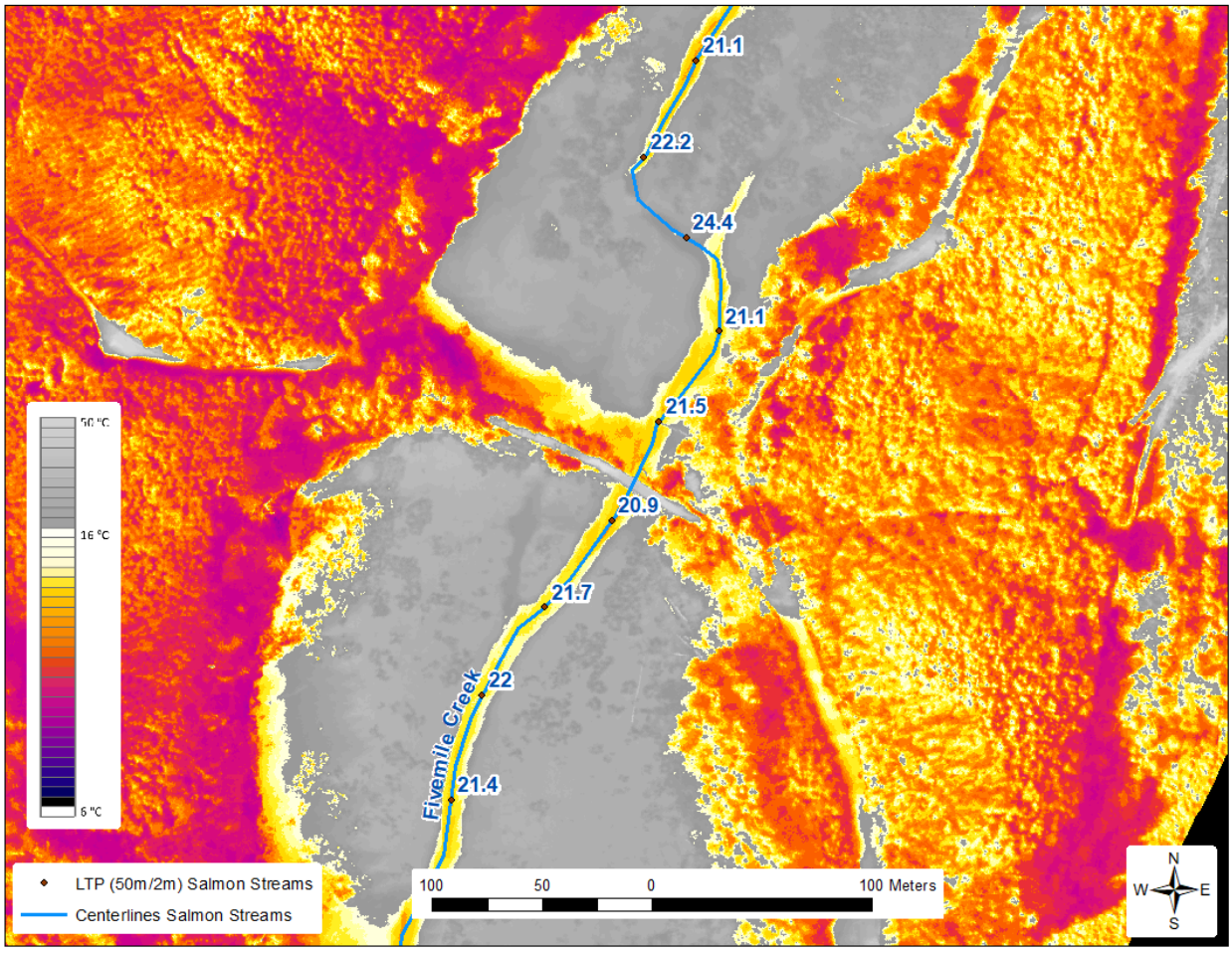

Figure 34: LTP overlayed on top of TIR data of Fivemile Creek at river km 0.55. This figure shows a continuous thermal signature of the active channel at the lower end of the surveyed area. The plot shows median water temperature (°C).

True Color Orthophoto Accuracy Assessment

A total of 14 Air Target Points (ATP) were collected throughout the Salmon Streams study area. ATPs were used along with automatically generated tie points and camera calibration information to adjust all images in 7 block using analytical aerial triangulation. Three air target points were withheld from the aerial triangulation as independent check points. These points were found in the adjusted orthophotos and the displacement was recorded for further statistical analysis. Due to the limited amount of ground control, photo accuracy results were computed on a cumulative basis instead of by photo block. Table 17 presents the complete photo accuracy statistics of both check points and control points (used in the aerial triangulation).

Table 17: Orthophotography accuracy statistics for Salmon Streams

Parameter	Units	Check Points$_x$	Check Points$_y$ n -= 3	Check Points$_{xy}$	Control Points$_x$	Control Points$_y$ n = 11	Control Points$_{xy}$
Mean	*m*	-0.014	0.042	0.044	-0.005	0.027	0.028
RMSE	*m*	0.044	0.058	0.073	0.033	0.038	0.050
1σ	*m*	0.052	0.049	0.071	0.034	0.027	0.043
1.96σ	*m*	0.101	0.096	0.139	0.066	0.053	0.085